Stability, Control and Performance for an Inverted Delta Wing-In-Ground Effect Aircraft

Submitted by:
Lee Qihui

Department of Mechanical Engineering

In partial fulfillment of the requirements for the Degree of Bachelor of Engineering
National University of Singapore

Session 2005 / 2006

Summary

The objective of this project is to investigate the Wing-In-Ground (WIG) effect on an Inverted Delta Wing configuration aircraft. It involves the study of aerodynamics and stability characteristics on a model aircraft, using both software simulation techniques and actual hardware testing. It encompasses a multidisciplinary effort to design, build and perform testing on an actual ground effect model aircraft.

This project can be broadly categories into 3 major milestones, which are all successfully achieved at the end of the project, and they are:

1) Design and simulations using computational and 3-D engineering software
2) Fabrication and experimental testing for stability and control
3) Actual flight testing under various conditions

The project began with reviews on the work done on WIGs and Inverted Delta wings. This was then accompanied by the theoretical study on the flight mechanics of WIG, as well as aerodynamic theory to calculate the forces and moments acting on the model aircraft and its control surfaces. Stability criteria were also reviewed and taken into considerations. Equipped with this knowledge, the aircraft was designed and a control system was planned with the objective of attaining static and dynamic flight stability, flight manoeuvrability and automatic height control. This involves developing the transfer functions of the various control components through self-designed experiments. Simulations were done to verify the accuracy of the preliminary design, and the various control system components were tested rigorously again to determine their respective characteristics. Based on the design made, a model aircraft was then built and a detailed stability and control analysis was carried out. This was done through a series of experiments, to test the model for its stability and control effectiveness, before actual flight tests. Finally, the performance of the aircraft was evaluated using both land and water testing, conducted over a 2 months period, which serve to verify its flight capabilities. The aircraft demonstrated great versatility in

its control and maneuvering during the numerous field tests conducted, justifying the effectiveness of the control system. In addition, the automatic height control function was able to stabilize the plane at the ideal flying height and provide accurate measurements of flight altitude and flight time.

In the short 9 months, the project team had successfully attained the initial objectives of designing, analyzing, fabricating and achieving a working Inverted Delta WIG aircraft. A simple project overview is presented in the flowchart on the right. The stability theory, control system and test flight results were also presented at the NUS Centennial Open House 2006.

Project Overview

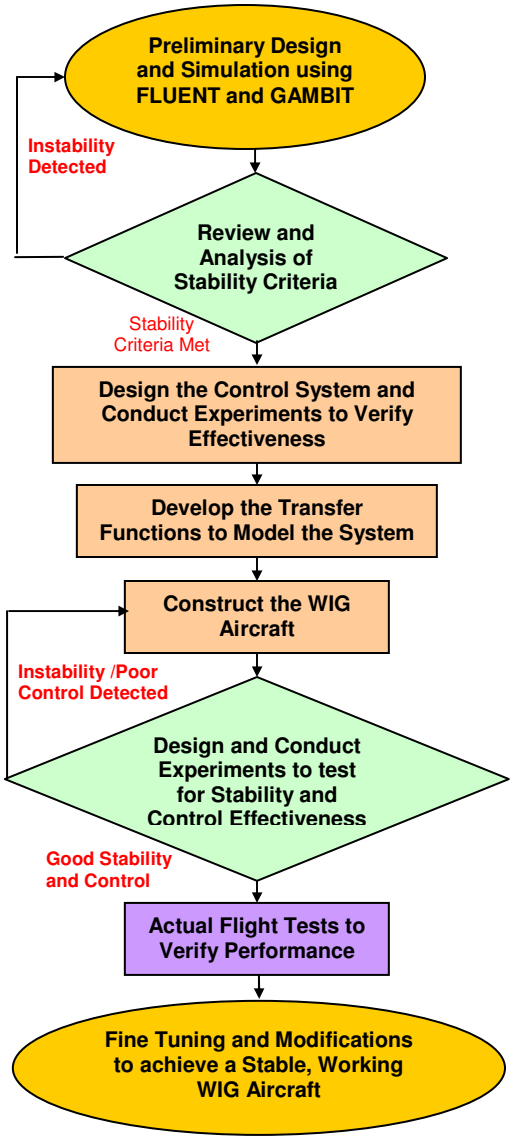

In conclusion, the project has successfully demonstrated the capabilities of an Inverted Delta WIG aircraft and its immense potential in the field of high speed marine transport, for both commercial and military usage. Useful insights are also gained on the fabrication and performance of a small scale WIG aircraft.

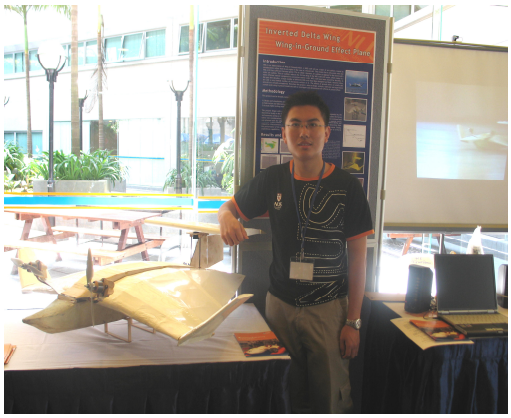

This project was done in collaboration with a fantastic friend and teammate, Mr Jiang Junde who was responsible for the aerodynamics and propulsion components of this assignment.

Acknowledgement

The author wishes to express his thanks and heartfelt gratitude to the following persons for their various contributions and important assistances rendered during the project.

- A/P Gerard Leng Siew Bing, Project Supervisor, for providing the necessary guidance and invaluable advice throughout the course of the project.
- Mr Jiang Junde, Project Member and Friend, for his contribution and effort in the aerodynamic and propulsion analysis.
- Mr Ahmad Bin Kasa, Ms Amy Chee, Ms Priscilla Lee and Mr Cheng Kok Seng, Staff of the Dynamics & Vibration lab, for their help and support during the project.
- Mr Kam Mun Loong, Mr Tan Han Yong, Mr Oi Tze Liang and Mr Teoh Wei Lit, PHD and Masters Students of COSY lab, for their help and encouragement.
- Mr Tan Gee Boon, Nicholas and Mr Ng Kah Yong, Filming Crew and Friends, for providing relentless assistances in filming the various test flights.
- Ms Lim Weiyee, Web page Designer and Friend, for her help in designing and developing the website for this WIG project.

Table of Contents

List of Figures

List of Tables

LIST OF SYMBOLS

c	Chord Length
č	Mean Chord Length
h	Height
h/c	Height to Chord Ratio
C_L	Coefficient of Lift
C_D	Coefficient of Drag
C_M	Coefficient of Moment
α	Angle of Attack
θ	Pitch Angle
δ_E	Angle of Deflection of Elevator
δ_R	Angle of Deflection of Rudder
x_{cp}	Center of Pressure
$x_{a/c}$	Aerodynamic center
x_θ	Aerodynamic center of Pitch
x_h	Aerodynamic center of Height
X_{CG}	X-Coordinate of C.G, with origin at Point A
Y_{CG}	Y-Coordinate of C.G, with origin at Point A
Z_{CG}	Z-Coordinate of C.G, with origin at Point A
b	Wing Span
AR	Aspect Ratio
Re	Reynolds Number
U	Reference Velocity / Free Stream Velocity
l	Reference Length
v	Kinematics Viscosity
ρ	Density
q	Pitch Rate
$C_{M\alpha}$	Derivative of the Coefficient of Moment With Respect To Angle of Attack
C_{M0}	Y intercept of the Coefficient of Moment
$C_{L\alpha}$	Derivative of the Coefficient of Lift With Respect To Angle of Attack

C_{Mh} Derivative of the Coefficient of Moment With Respect To Height

C_{Lh} Derivative of the Coefficient of Lift with Respect To Height

C_{Mwf} Characteristic Curve of the Coefficient of Moment for Wing-Fuselage Combination

C_{Mt} Characteristic Curve of the Coefficient of Moment for Tail

C_{Mwft} Characteristic Curve of the Coefficient of Moment for Wing-Fuselage-Tail Combination

V_H Tail Volume Ratio

$C_{M\alpha t}$ Derivative of the Coefficient of Moment of the Tail With Respect To Angle of Attack

C_{M0t} Y Intercept of the Characteristic Curve of the Coefficient of Moment of the Tail

$C_{L\alpha t}$ Derivative of the Coefficient of Lift of the Tail With Respect To Angle of Attack

ε Downwash Angle

i_w Wing Angle of Incidence

i_t Tail Angle of Incidence

l_t Distance between the C.G and a/c of tail

S_t Area of tail

η Tail efficiency

τ Control Surface effectiveness parameter

M_p Maximum Overshoot

t_s Settling Time

t_r Rise Time

ξ Damping Ratio

ω_n Natural Frequency

1 Introduction

WIG is an abbreviation for Wing In Ground-effect. A WIG aircraft takes advantage of this ground effect phenomenon, where an aircraft flying at low altitudes close to the ground (h/c between 0.05 - 0.25), experience an increase in lift on the wings, while drag decreases. This results in an enhanced lift-to-drag ratio (as shown in Figure 1 below where readings are obtained through CFD simulations) and hence greater flight efficiency. A WIG aircraft sits on a layer of dynamic air cushion created by aerodynamics as a result of sufficient forward speed, rather than static air cushion produced by an engine like in the case of a hovercraft. This air cushion reduces the friction drag of the WIG craft on water, which makes it a more efficient vehicle compared to convention marine craft. WIG aircraft have been around for decades. In the past few years, a large number of different WIG aircraft have been designed and built. However there are very limited literatures written on it, especially on an Inverted Delta wing configuration. Many of the existing results published in journals are based on experiments done on large scale WIG aircraft, while ground effect phenomenon on small-scale aircraft is virtually unexplored. Furthermore, little study has been done to investigate the effect of an Inverted Delta wing configuration, despite its apparent advantage of enhanced performance and better stability. As such, this project aims to provide an insight into this unknown and niche area of aerodynamics, by designing, analyzing, fabricating and experimenting on a small scale Inverted Delta WIG model. This serves to investigate and demonstrate the ground effect phenomenon, and how the Inverted Delta wing configuration contributes to overall stability and enhances performance.

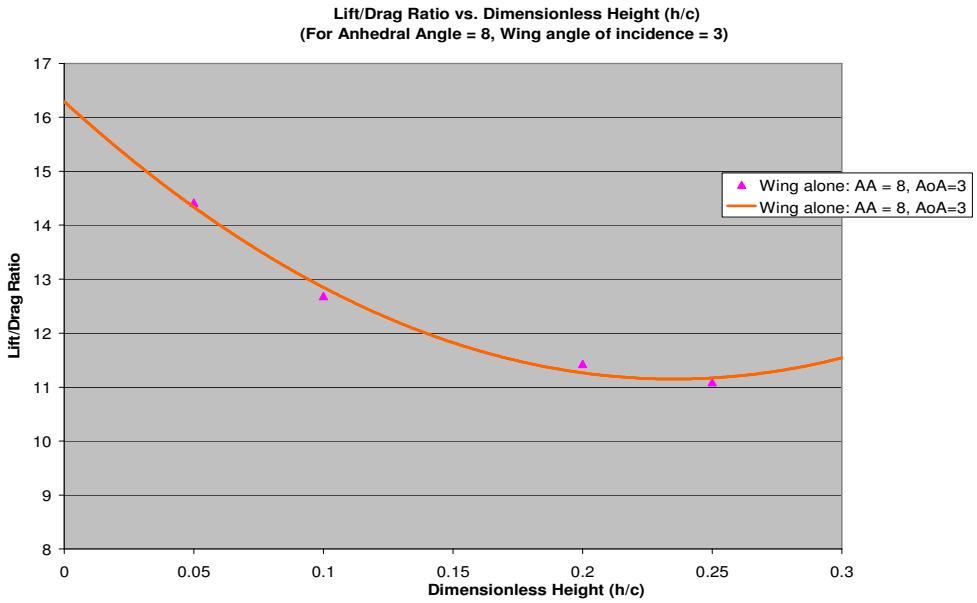

Figure 1: Graph showing L/D ratio increasing as h/c decreases

This project is a joint effort of 2 final year students covering the areas of aerodynamics, propulsion, stability and control. In this thesis, the stability and control aspects of the WIG aircraft will be discussed and presented.

1.1 Project Objectives

The following objectives are to be achieved:

- Literature review and theoretical study of WIG aircraft's dynamics, stability and control.
- Understanding of the Inverted Delta wing configuration
- Stability analysis of the WIG aircraft.
- Stability experiments designed and performed on the WIG aircraft.
- Design, analysis and experimental testing of the individual control components.
- Integration and experimental testing of the complete control system.
- Test flight of the fabricated prototype.
- Verification of theoretical results against actual flight performance

1.2 Structure of the Dissertation

This thesis is divided into 8 Chapters and they are organized as follows:

Chapter 2 – Literature Review on a short history of WIG aircraft and their potential area of applications.

Chapter 3 – Discusses the theoretical stability criteria for a WIG aircraft. It includes pitch and height static stability criterions and dynamic stability considerations.

Chapter 4 – Describes the stability analysis done on the aircraft. It presents CFD simulation results and describes the designing of a horizontal tail stabilizer. This section also includes the experiments conducted to find the C.G. of the aircraft and to align the motors' thrust lines.

Chapter 5 – Determines the aerodynamic control of the WIG aircraft. It describes the design of the control surfaces, sizing of the control electronics and the analysis of their effectiveness. Experiments were performed on individual control components to determine their characteristics. This is necessary to allow successful integration of the control system into the WIG aircraft.

Chapter 6 – Discusses the theoretical designing and analysis of an automatic height control system. This includes hardware selection and testing, software coding and the determination of aerodynamics transfer function. A block diagram model representing the entire height control system is derived.

Chapter 7 – Discusses the flight tests conducted under various conditions, and performance evaluation. The automatic height control system is also examined

Chapter 8 – Project conclusion and recommendations for further study

2 Literature Review on WIG Aircraft

The project began with the study of relevant journals, articles and reference texts documenting the various aspects of WIG aircraft. In addition, thesis done by previous student on a rectangular wing model WIG aircraft was also examined. This is to allow for an appreciation of the advantages of a WIG aircraft and its potential area of applications; and develop an understanding of aerodynamics theory and the various design considerations for achieving flight stability and control.

2.1 History of WIG Aircraft

Wing in Ground (WIG) vehicles, or sometimes referred to as Ekranoplans, have enormous applications in several areas. These areas include cargo transportation, military operations and even search and rescue missions. The main reason for the development of WIG aircraft is due to the speed limitations of conventional marine craft. The practical maximum speed of all marine craft mentioned so far lies around 100 km/h. The drawback for high speed marine craft is the increased power requirement and fuel consumption. This is caused by increased viscous drag due to water friction. The obvious solution is to minimize contact with the water surface during cruise conditions. This approach works for hydrofoils and hovercraft. Unfortunately, the speed of a hovercraft is bounded by the sea state and longitudinal stability considerations; and the speed of a hydrofoil by cavitations of the foils.

Early experiments of ground effect vehicles were conducted using models and small scaled prototypes. The best known inventor's application for a surface effect vehicle belongs to the Finnish engineer G. Kaario (1935). He built a craft which was shaped out of a snow plane in the shape of a ski supporting small elongation wing. Early tests showed positive ground effect. However the project was halted as he could not solve the instability problem. Similar works were

carried out by the Swedish and American engineers. However stability problems plagued their experiments and therefore could not produce any practical prototypes. Little was known about the control systems for early ground effect vehicles.

In 1947, a Russian scientist, R.Alekseev made proposals on aerodynamic forces acting on the motion of high speed craft near the surface. His proposals were based on the principles of provision of longitudinal and lateral stability near the surface. It was through these principles that he was able to design and built the first workable prototype of a WIG aircraft or Ekranoplan. Designs were initially based upon the tandem wing which was later replaced by the more favorable "plane" type configuration. This resulted in the production of well-known Ekranoplans such as the "Lun", the "Orlyonok" and the most famous of all the "KM" or "Korabl' Maket", also known as the Caspian Sea Monster. Weighing at a staggering 500 tons, this craft is capable of reaching speeds of up to 500km/hr.

Figure 2: KM Ekranoplan – 'Caspian Sea Monster'

Stability was attained by the inclusion of an enormous horizontal tail. This aids in counteracting any excessive, unwanted moments. It provides longitudinal trim, stability and controllability.

Incorporated into this enormous aircraft was a system which provided controls for the elevator, rudder, wing flaps and hinge nozzles. An automatic control system was used to control the damping and stabilizing of flight altitudes, pitch angle and speed. With regards to longitudinal stability issues due to ground effect, the WIG aircraft requires a multi dimensional control system. As such, piloting a ground effect aircraft is still extremely challenging, with narrow margins for errors.

However, following the collapse of the Soviet Union, developing and maintaining big ekranoplans became impossible for the Russians and the design bureaus started focusing on smaller ekranoplans for non-military use. In recent years, the WIG effect technology has caught the interest of many parties. A few years back, Boeing Phantom Works announced a project to develop a high-capacity cargo plane utilizing ground effect for military and commercial purposes. Success was also seen in the recent development of Airfisch and FS8 WIG aircrafts, designed by German firm AFD. Even locally in Singapore, there have been interests shown by engineering companies to design and market commercial WIG aircrafts. This was the reason why Widgetworks PTE LTD started its collaboration with NUS to fund projects investigating WIG effect.

Figure 3: Airfisch (Left) and FS8 (Right)

2.2 Potential Benefits and Applications of WIG Aircraft

As a means of transportation, WIG aircraft is well positioned in the niche between ships and conventional aircraft. Speeds of WIG (up to 500 km/hr) are much higher than those of high speed ships (typically about 80 km/hr), while operational expenses are much lower than that of airplanes. In addition, most

WIG aircrafts display amphibious properties and can take off and land on any relatively flat surfaces, such as land, water, snow and ice. As such, in recent years, there have been increased interest and research effort put into developing WIG aircraft for both commercial and military purpose. The following are some potential benefits and possible applications for WIG aircraft:

- WIG craft can fulfill the need for increased speed of marine transport and fill the gap between shipping and aviation. It offers itself as a potential substitute for high speed trans-island transport or international cargo shipping.
- WIG craft is able to achieve high speeds, while maintaining increase efficiency and improve lift-to-weight ratio, especially when compared to other high speed marine craft. This allows WIG aircraft to carry more loads and cover greater distance, providing enhanced fuel efficiency.
- WIG craft can fly below air defence radars' zone and are invulnerable to mine-torpedo weapons. This offers great military application potential for transporting troops or logistic supplies.
- Due to the marine nature of WIG craft, its operating and maintenance cost is lower when compared to conventional airplane.
- The infrastructure requirements for WIG craft are very low. Any existing port facilities are sufficient.
- Especially in a wavy sea, the comfort level in cruise for WIG craft is very much higher when compared to other high speed marine craft.

3 Establishing the Stability Criteria of WIG Aircraft

One major aspect of designing a WIG aircraft is to understand, evaluate and determine its stability criteria. In this section, the various stability criteria will be discussed, and this forms the basis on which the subsequent stability analysis of the model WIG aircraft will be based upon.

3.1 Static Stability

Stability is a property of an equilibrium state. That is, if the aircraft is to remain in steady uniform flight, the resultant force and resultant moment about the C.G must both be equal 0 as shown in Figure 4. An aircraft satisfying this requirement is said to be at trim condition. On the other hand, if the forces and moments do not sum to 0, the airplane will be subjected to translational and rotational accelerations, resulting in instability.

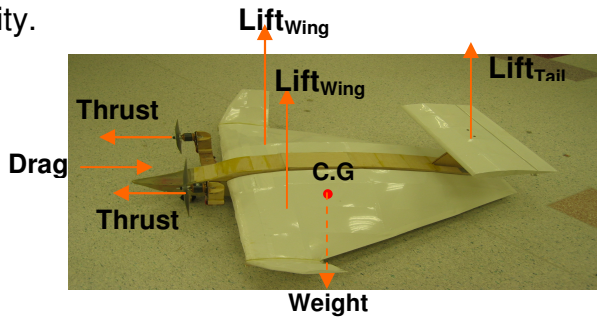

Figure 4: Forces acting on the WIG aircraft

The subject of stability is generally divided into static and dynamic stability. Static stability refers to the initial tendency of the aircraft to return to its equilibrium or trim state after a disturbance. If there exists a natural tendency for the aircraft to generate a restoring force or moment to return to its equilibrium point, then the aircraft is said to be statically stable.

3.1.1 Longitudinal Static Stability

Longitudinal static stability of the WIG aircraft is extremely sensitive to both pitch and height variations. This is quite different from conventional aircraft where changes in

height results in minimal force and moment variations, and as such, is ignored and only requires consideration for pitch stability.

However, in the presence of ground effect, force and moment acting on the aircraft change with both pitch and height. Therefore, both pitch and height stability considerations must be taken. A WIG aircraft has two aerodynamic centers. The *center of pitch* $\mathbf{x_\theta}$ follows conventional aerodynamics definition and is where the moment acting on the body is independent of the angle of attack. Similarly, the *centre of height* $\mathbf{x_h}$ is defined as the point where moment is independent of flying height. These two aerodynamic centers can be obtained by considering the Lift and Moment curve with respect to angle of attack and with respect to height.

Pitch Stability Criterion:

For pitch stability, the required conditions are well illustrated in the following diagram.

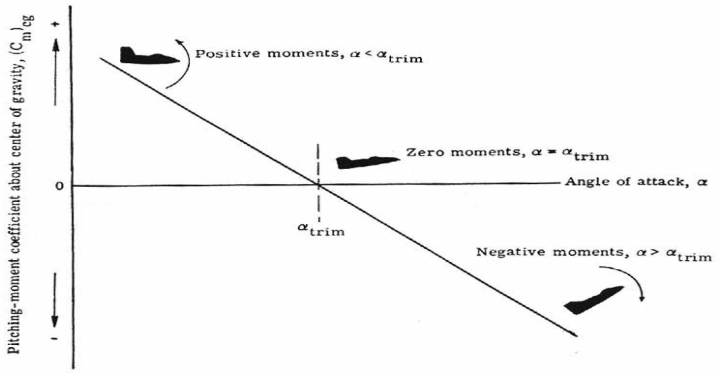

Figure 5: Ideal pitching moment curve and equilibrium condition

At trim condition, the aircraft is at equilibrium and flying at an angle of attack, where there are no moment tendencies to pitch the aircraft about its C.G. At angle of attack less than α_{trim}, the aircraft creates a positive (nose-up) moment that would rotate it back towards the equilibrium point. On the other hand, if the aircraft experiences a disturbance, such as a sudden upward gust, that increases the angle of attack to greater than α_{trim}, a negative (nose-down) moment will develop and tend to rotate it back to the equilibrium. On the basis of this simple analysis, to have static pitch

stability, the aircraft pitching moment curve must have a negative slope and intercept the positive Y-axis.

$C_{M\alpha} < 0$ (1)

$C_{M0} > 0$ (2)

Height Stability Criterion:

By Routh – Hurwitz Criteria, the condition of height stability for a WIG aircraft can be mathematically expressed as:

$\Delta X = X_\theta - X_h > 0$ (3)

Where $(X_{CG} / č - X_\theta / č) = C_{M\alpha} / C_{L\alpha}$

$(X_{CG} / č - X_h / č) = C_{Mh} / C_{Lh}$

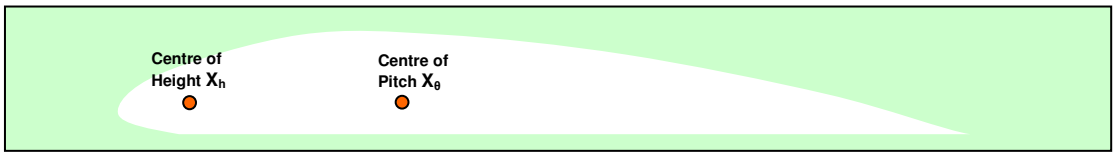

Figure 6: Relative position of aerodynamic centres for stability

That is to say, the final configuration of the aircraft must be such that the aerodynamic center of height is located upstream of the aerodynamic center of pitch. In addition, research results show that the ideal ΔX should be between 0.05 - 0.20č. If $\Delta X > 0.20č$, then the static stability becomes excessive leading to dynamic instability. On the other hand, if $\Delta X < 0.05č$, then there is insufficient stability which can lead to long-period (phugoid) fluctuations.

C.G Positioning:

The location of the C.G. is crucial for establishing acceptable longitudinal stability as it affects the dynamics of the aircraft. Sensitivities of the pitch angle and flight altitude to changes in velocity are important for determining an ideal C.G position. The derivative of pitch angle with respect to velocity can be shown to be:

$d\theta / dU = -2/U \, [C_L / (dC_L / d\theta)] \, [X_h / (X_\theta - X_h)]$ (4)

Similarly, the derivative of flight altitude with respect to velocity is:

$$dh/dU = 2/U\,[C_L / (dC_L / dh)]\,[X_\theta / (X_\theta - X_h)] \qquad (5)$$

Looking at equation (4), if the aerodynamic centre of height coincides with the C.G position, then X_h, when measured with respect to C.G, is zero and the pitch angle will not vary with velocity. If C.G is between the aerodynamic centre of height and centre of pitch, then $X_h < 0$ and $(X_\theta - X_h) > 0$; and the pitch angle will decrease with increasing velocity as seen in equation (4). Furthermore, according to equation (5), when C.G is between the two aerodynamic centres, $X_\theta > 0$ and the term $[X_\theta / (X_\theta - X_h)] < 1$, this will lead to an increase in damping effect and is desirable. On the other hand, if C.G is in front of both aerodynamic centres, then $X_h > 0$, $X_\theta > 0$ and $[X_\theta / (X_\theta - X_h)] > 1$, which represent a decrease in damping effect and an increase in height variation with velocity. Therefore, to achieve stability, C.G should be located between the two aerodynamic centres, and placed close to the centre of height, as expressed in equation (6) below.

$$X_h < X_{CG} < X_\theta \text{ and } X_{CG} \sim X_h \qquad (6)$$

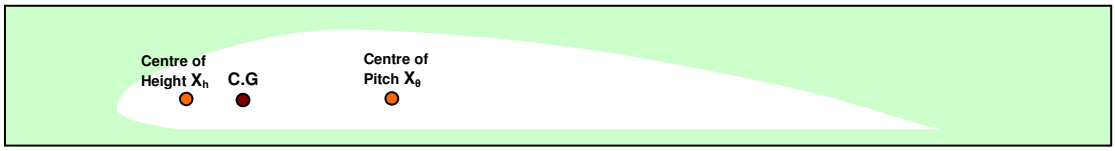

Figure 7: Relative position of aerodynamic centres and CG for stability

3.1.2 Lateral Static Stability

Lateral stability refers to stability in the roll axis. An aircraft possesses static roll stability if a restoring moment is developed when it is disturbed from a wings-level attitude. When a WIG aircraft is rolled, the pressure on its lifting surfaces changes and is redistributed. Part of the lifting elements approaches the ground and hence experiences an increase in lift; while the other part deviates from it with a resulting decrease in lift. This situation causes the generation of a recovering moment that

brings the aircraft back to wing level. In addition, by adopting a high wing configuration, there will be a stabilizing roll moment created by the flow around the fuselage. Therefore a WIG aircraft, unlike a conventional airplane, has a natural aerodynamic stabilization of roll angle in flight. This is an extremely important aspect of flight safety.

3.2 Dynamic Stability

The study of dynamic stability focus on the time response of motion of the aircraft after it is disturbed from its equilibrium point and is determined by the character of this disturbed motion. It examines important parameters such as frequency and period of motion, damping ratio and settling time. If the disturbance reduces with time, it indicates that there is resistance to the motion and therefore energy is dissipated. The dissipation of energy is called positive damping. On the other hand, if energy is being added to the system, then it is known as negative damping. Positive damping for an aircraft is provided by forces and moments that arise due to the aircraft's motion. This positive damping will oppose the motion of the aircraft and cause the disturbance to damp out over time. How long it will take for the system to settle down will depend on the damping ratio. An aircraft that has negative aerodynamic damping will be dynamically unstable. It is important to note that an aircraft can be statically stable but dynamically unstable. Static stability, therefore, does not guarantee dynamic stability.

3.2.1 Longitudinal Dynamic Stability

To ensure longitudinal dynamic stability, the C.G of the WIG aircraft should be located within a certain range, as specified in equation (6).In addition, it is important to understand the equation of pitching motion of the WIG aircraft to determine the time response, when it is subjected to external disturbances or changes in control input. If the aircraft is able to stabilise and achieve steady state, rather than go into an extended state of fluctuation, then it is dynamically stable. The pitching moment equation and aircraft transfer function will be derived in chapter 6 of this report.

4 Stability Analysis

Following the theoretical studies of stability criteria, it is vital to ensure that these conditions are implemented in the model aircraft as accurately as possible. Before any flight testing can commence, it is important to conduct laboratory based experiments on the completed aircraft to analyse and verify that necessary stability conditions are indeed fulfilled. This will help to ensure good flight performance and minimise instability.

4.1 Initial Analysis

CFD simulations are initially done on Wing alone and Wing + Hull configurations to obtain a series of force and moment readings. The moment characteristics curves plotted, for both configurations, are upward sloping and intercept the negative Y-axis as shown in Figure 8 below. Based on stability theory shown in equation (1) and (2) earlier, this represents an inherent instability.

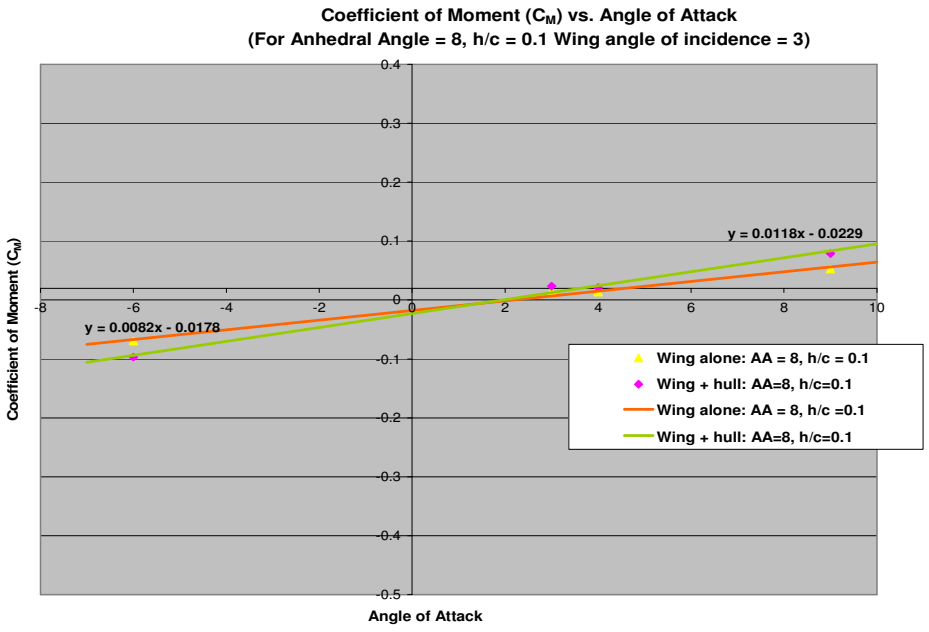

Figure 8: Moment characteristic curves of Wing alone (orange curve) and Wing + Hull (green curve) configurations

In addition, considering the Wing + Hull configuration, the centre of pitch and centre of height are found to be:

Given that centre of gravity, $X_{CG} = 0.28č$, where č = 0.535cm

$(X_{CG} / č – Xθ / č) = C_{Mα} / C_{Lα} = 0.0118 / 0.0696 = 0.170$
$\mathbf{X_θ}$ = (0.280 – 0.170) č = 0.110č = **0.059 m from leading edge**

$(X_{CG} / č – Xh / č) = C_{Mh} / C_{Lh} = -0.0654 / -0.6362 = 0.103$
$\mathbf{X_h}$ = (0.280 – 0.103) č = 0.177č = **0.095 m from the leading edge**

This shows that the centre of height is aft of the centre of pitch ($\Delta X = Xθ – Xh < 0$), and thus, the height stability criterion as stated in equation (3) is not met. This results in instability.

Lastly, the ideal C.G position of 0.28č (0.15m) from the leading edge is not between, but instead, behind the two aerodynamic centres. This contributes to the instability of the aircraft.

4.2 Designing the Horizontal Tail

To correct this instability problem, a horizontal tail stabilizer needs to be introduced to create a correcting moment that can balance the aircraft and help attain trim condition. The horizontal tail will also help to shift the centre of pitch downstream.

In designing the horizontal tail stabilizer, several parameters have to be considered. This includes the airfoil data, span and chord dimensions, aspect ratio, distance of the tail from the C.G position and tail angle of incidence. The whole design process begins with making an estimation of the ideal pitching moment characteristic curve required from the whole aircraft. From earlier

simulations, it is determined that the ideal trim condition for the aircraft should occur at an angle of attack of approximately 4°. This is because at this angle, the wings are able to generate the necessary lift required to carry the design payload. Furthermore, the positive Y-intercept for the moment curve is set at 0.06. This is to satisfy the stability criteria. As such, the ideal moment equation is:

$$\mathbf{C_{M\alpha\ wft} = -\ 0.015\ \alpha + 0.06}$$

Considering the moment characteristic curve for the Wing + Hull configuration which is found to be:

$$\mathbf{C_{M\alpha\ wf} = 0.0118\ \alpha - 0.0229}$$

Therefore, the tail must contribute:

$$\mathbf{C_{M\alpha\ t}} = C_{M\alpha\ wft} - C_{M\alpha\ wf} = -0.015 - 0.0118 = \mathbf{-\ 0.0268}\ /°$$

$$\mathbf{C_{M0\ t}} = C_{M0\ wft} - C_{M0\ wf} = 0.06 - (-0.0229) = \mathbf{0.0829}$$

The pitching moment due to the tail can be approximated by the following equation:

$$M_t = -\ l_t L_t = -\ l_t\ C_{Lt}\ 0.5\ \rho\ U_t^2 S_t \qquad (7)$$

$$C_{Mt} = M_t / (0.5\ \rho\ U^2\ S\check{c}) = -\ (l_t\ S_t / S\check{c})\ \eta C_{Lt} = -\ V_H\ \eta C_{Lt} \qquad (8)$$

The Coefficient of Lift for the tail can be written as:

$$C_{Lt} = C_{L\alpha t}\ \alpha_t = C_{L\alpha t}\ (\alpha_w - i_w - \varepsilon + i_t) \qquad (9)$$

The downwash angle can be expressed as:

$$\varepsilon = \varepsilon_0 + d\varepsilon/d\alpha_w \ \alpha_w \qquad (10)$$

where ε_0 is the downwash at zero angle of attack

The downwash behind a wing can be derived from the finite-wing theory and shown to be related to the wing lift coefficient and aspect ratio:

$$\varepsilon = 2C_{Lw} / \pi AR_w \qquad (11)$$

The rate of change of downwash angle with angle of attack is determined by taking derivative of equation (10):

$$d\varepsilon/d\alpha_w = (2C_{L\alpha w} / \pi AR_w) \qquad (12)$$

Now, rewriting the tail contribution to the pitching moment by substituting equation (9) and (10) into equation (8) yields:

$$C_{Mt} = \eta V_H C_{L\alpha t} (\varepsilon_0 + i_w - i_t) - \eta V_H C_{L\alpha t} \alpha(1 - d\varepsilon/d\alpha_w) \qquad (13)$$

Comparing equation (10) with the linear expression for the tail pitching moment characteristic curve,

$$C_{Mt} = C_{M0\,t} + C_{M\alpha\,t}\,\alpha$$

yields expressions for the slope and the Y- intercept:

$$C_{M0\,t} = \eta V_H C_{L\alpha t} (\varepsilon_0 + i_w - i_t) \qquad (14)$$

$$C_{M\alpha\,t} = - \eta V_H C_{L\alpha t} (1 - d\varepsilon/d\alpha_w) \qquad (15)$$

As seen from equation (14), the tail contribution to C_{M0} is positive and can be used to ensure that the overall C_{M0} of the WIG aircraft intercept the positive Y-axis, as required for stability. This can be accomplished by adjusting the tail incidence angle i_t. In addition, equation (15) shows that the tail should contribute a negative gradient moment curve to the overall moment characteristic of the entire WIG aircraft and help to enhance stability. This can be controlled by proper selection of V_H and $C_{L\alpha t}$. The contribution of $C_{M\alpha\ t}$ will become more negative by increasing the tail moment arm l_t or tail surface area S_t and by increasing $C_{L\alpha t}$. The tail lift curve slope $C_{L\alpha t}$ can be increased most easily by increasing the aspect ratio of the tail platform.

To simplify the design process, the following parameters are first estimated and set:

- **Aspect Ratio $_{tail}$ = $(b/c)_t$ = AR_t = 2.2**
- **Tail moment arm, l_t = 0.465 m**
- **Tail efficiency, η** = 0.5 ρ U_t^2 / 0.5 ρ U_w^2 = **1**
- **$C_{L\alpha t} \approx C_{L\alpha\ w}$ = 0.0559** /°

Note that: $C_{L\alpha\ w}$ and $C_{L0\ w}$ are obtained from the Lift vs Angle of Attack (Wing Alone configuration) curve.

From equation (12):

$d\varepsilon/d\alpha_w$ = $(2C_{L\alpha w} / \pi\ AR_w)$ = 2 (0.0559/°) / π (1.98) = **0.0178**

From equation (15), solving for the tail volume ratio:

$V_H = - C_{M\alpha\ t} / [\eta\ C_{L\alpha t} (1 - d\varepsilon/d\alpha_w)]$

Substituting all the relevant values gives:

V_H = - (-0.0268 /°) / [(1) (0.0559 /°)(1 – 0.0178)] = **0.488 m^3**

The horizontal tail volume ratio is expressed as

$V_H = (l_t S_t / S\check{c})$
and solving for the horizontal tail area yields:

$\mathbf{S_t}$ = (0.488) (0.250) (0.535) / 0.465 = **0.140 m^2**

Setting AR_t = 2.2,

b_t / c_t = 2.2

$S_t = c_t$ x 2.2 c_t = 0.140

Therefore, $\mathbf{c_t}$ = **0.252 m** and $\mathbf{b_t}$ = 2.2 x ct = **0.554 m**

This is the tail configuration needed to provide the required tail contribution to $C_{M\alpha}$, so that the ideal moment curve is achieved.

Next is to determine the tail angle of incidence. From equation (14):

$$i_t = -([C_{M0\,t} / \eta V_H C_{L\alpha t}] - i_w - \varepsilon_0) \qquad (16)$$

The only unknown in equation (16) is ε_0; that is, the downwash angle at the tail when the wing is at zero angle of attack. This can be estimated using equation (11):

$\boldsymbol{\varepsilon_0} = 2C_{L0\,w} / \pi AR_w = 2(0.0846) / \pi (1.98) =$ **0.027°**

Now solving for equation (16) gives:

$\mathbf{i_t}$ = - ([0.0829 / (1) (0.488) (0.0559)] – 3 – 0.027) = **0.012° ≈ 0°**

The calculations above provide the basic parameters on which the design, simulation and construction of the horizontal tail will be based upon.

To verify the performance of the horizontal tail design and justify the theoretical calculations made above, a series of CFD simulations is done to determine the lift and moment generated on the tail at various angles of attack. A GAMBIT model of the tail, that has been carefully meshed, is shown in Figure 9 below.

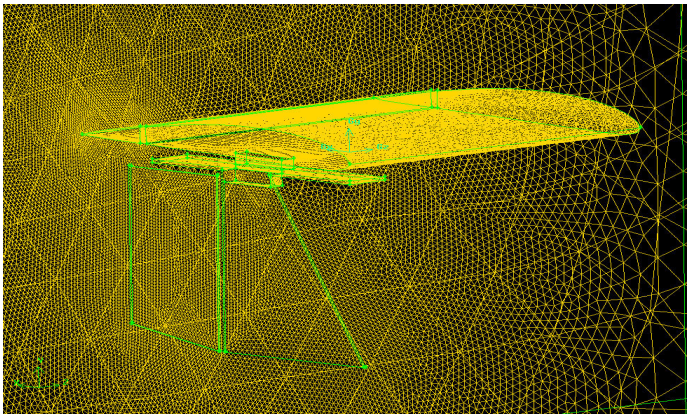

Figure 9: Gambit model of the horizontal tail stabilizer unit

The moment characteristic curve of the tail is then plotted (as seen in Figure 11) to ensure that the simulations readings are in close accordance to the theoretical results obtained above. From the plotted curve, the moment equation of the tail is found to be:

$$\mathbf{C_{M\alpha\ t} = -\ 0.0273\ \alpha + 0.0846}$$

This is very close to the theoretical equation $\mathbf{C_{M\alpha t} = -\ 0.0268\ \alpha + 0.0829}$ mentioned above.

Finally, the moment characteristic curve of the entire aircraft is plotted (as seen in Figure 11) using simulation results, to ensure that its gradient is negative and it intercepts the positive Y-axis, as required to satisfy longitudinal stability conditions. An example of the CFD static pressure contour plot of the aircraft is shown in Figure 10 below. From the plotted curve, the moment characteristic equation of the entire aircraft is found to be:

$$\mathbf{C_{M\alpha\ wft} = -\ 0.0156\ \alpha + 0.063}$$

Once again, this curve, obtained from simulation results, is found to be in close agreement to the theoretical equation $\mathbf{C_{M\alpha\ wft} = -\ 0.015\ \alpha + 0.06}$ stated before. Also note that the trim angle is approximately at 4° as specified earlier.

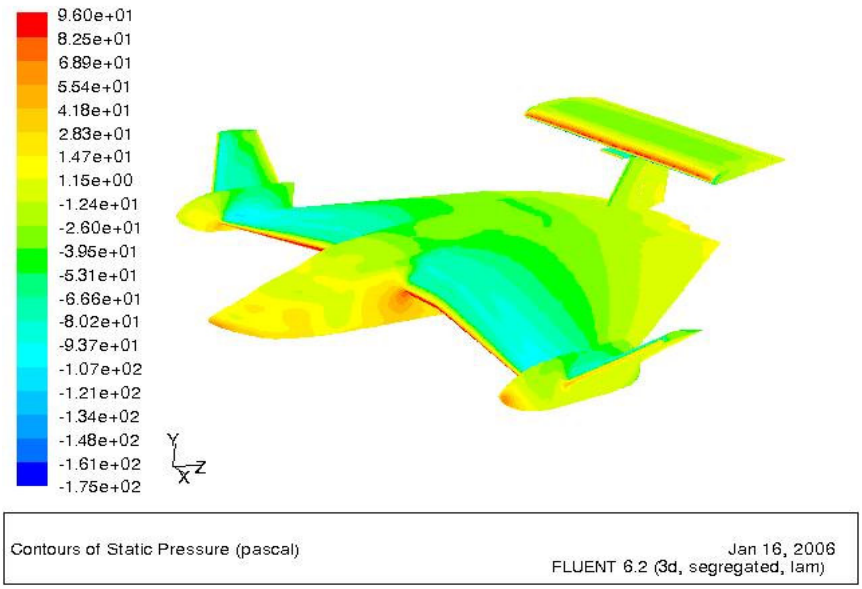

Figure 10: CFD static pressure contour plot of the entire WIG aircraft model

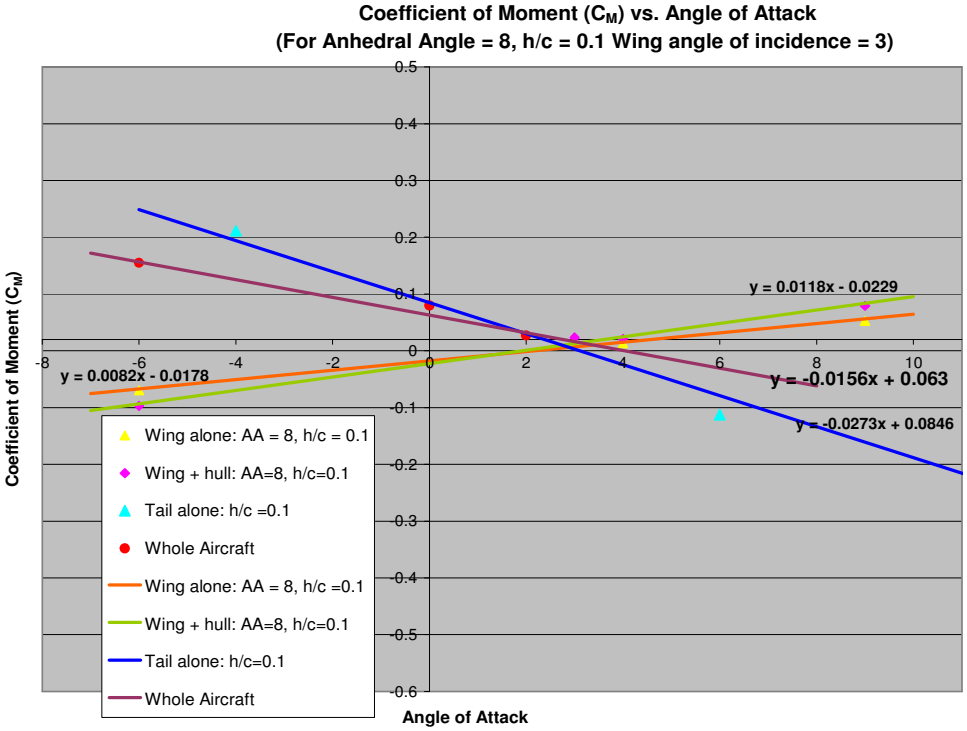

Figure 11: Moment characteristic curves of Wing alone (orange curve), Wing + Hull (green curve), Tail alone (blue curve) and Whole aircraft (maroon curve) configurations

As seen in Figure 11 above, following the addition of the horizontal tail stabilizer, the moment characteristic curve for the entire aircraft is now downward sloping and intercepting the positive Y-axis. The trim condition occurs at approximately 4° angle of attack as desired. This satisfies the pitch stability criteria established earlier.

In addition, the centre of pitch and centre of height are now found to be:
$(X_{CG} / \check{c} - X_{\theta} / \check{c}) = C_{M\alpha} / C_{L\alpha} = -0.0156 / 0.1274 = -0.122$
$\mathbf{X_{\theta}}$ = (0.280 + 0.122) č = 0.402č = **0.215 m from leading edge**

$(X_{CG} / \check{c} - X_{h} / \check{c}) = C_{Mh} / C_{Lh} = -0.0671 / -0.9862 = 0.068$
$\mathbf{X_{h}}$ = (0.280 – 0.068) č = 0.212č = **0.113 m from the leading edge**

From the above calculations, the aerodynamic center of height is now located upstream of the aerodynamic center of pitch and $\Delta\mathbf{X}$ is **0.19č**. Furthermore, the ideal C.G position (0.15m from the leading edge) is now in between the two aerodynamic centres. As such, stability conditions, as specified in equation (3) and (6), are now satisfied.

In summary, the level of longitudinal static stability can be controlled through proper selection of the horizontal tail, by manipulating the volume ratio. The parameters making up the volume ratio that can be varied is the horizontal tail surface area and distance between the C.G and a/c of the tail. In addition, the tail incidence angle can be adjusted to yield whatever C_{M0} needed to achieve the desired trim condition.

4.3 Determination of CG Position

As discussed earlier, the placement of the CG position is a major factor in ensuring stability. Based on above theoretical results, the aerodynamics centre of pitch and centre of height are found to be at 0.402č and 0.212č respectively. As

such, the CG position should ideally be between these two points and is fixed at 0.280č. Design and fabrication considerations are taken into an account to ensure that this position is achieved. After the fabrication has been completed, two separate experiments are conducted to verify that the C.G position is indeed at its ideal point as planned earlier.

4.3.1 Experiment 1 - Position Estimation

Using a commercial, off-the-shelf C.G balancing machine, the model aircraft is rested and balanced on the device to estimate an approximate region where the C.G position lies. The experimental setup is illustrated in Figure 12 below. This is to mark out the region of interest, in which the later experiment 2 will be focusing on, to determine the exact C.G location and its 3-dimensional coordinates.

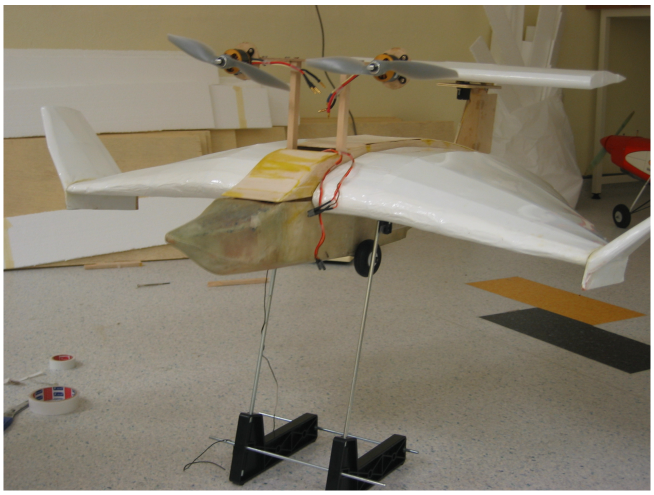

Figure 12: Model aircraft resting on the CG balancing machine

As seen above, the model aircraft with all its various components installed balances itself at the approximate C.G position when placed on the balancing machine. This helps to identify a rough region where the CG lies and the exact 3-dimensional coordinates will be determined in Experiment 2.

4.3.2 Experiment 2 -Determination of Exact Position

A series of experiment, based on simple force–moment theory, is designed to measure and calculate the exact coordinates of the C.G position.

Before the experiment, the total weight of the aircraft, **w** is found to be ***2.027kg***

Y-coordinate:

The experimental setup for calculating the Y-Coordinate of the CG position is illustrated in the following diagram and the table shows the readings obtained:

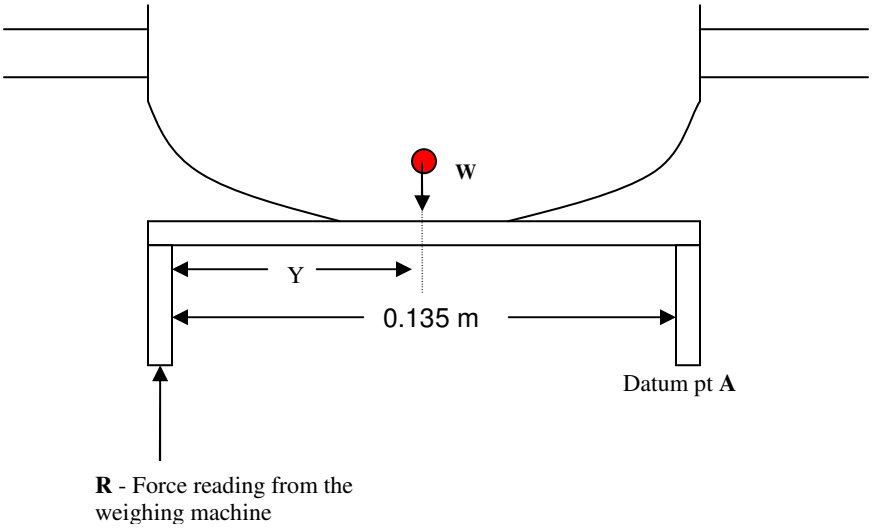

Figure 13: Free Body Diagram

Figure 14: Illustration of the Experimental Setup

Table 1: Readings from weighing machine for calculating X-Coordinate

R_1 /kg	R_2 /kg	R_3 /kg	R_{Avg} /kg	R_{FY}/N
1.276	1.280	1.277	1.278	***12.54***

Sample calculation:

Having known R_{FY} = **12.54N**, Y_{CG} can be determined by taking moment about point A:

Taking anticlockwise moment as +ve:

$\Sigma M_A = w\,(9.81)\,(0.135 - Y_{CG}) - R_{FY}\,(0.135) = 0$

$(2.027)\ (9.81)\ (0.135 - Y_{CG}) - (12.54)\ (0.135) = 0$

Y_{CG} = 0.050m (from the right edge of the hull)

X-Coordinate:

The experimental setup for finding the X-Coordinate of the CG position is illustrated in the following diagram and the table tabulates the readings obtained:

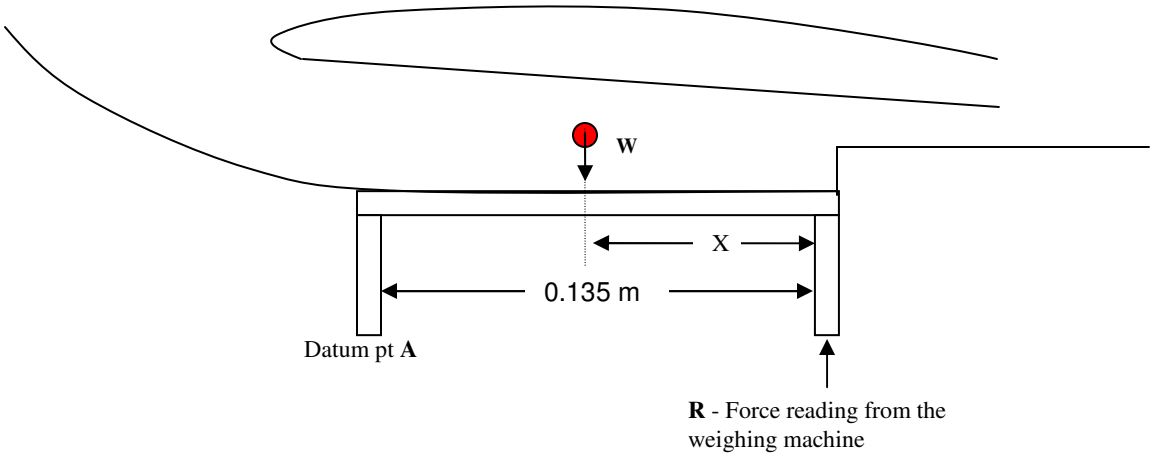

Figure 15: Free Body Diagram

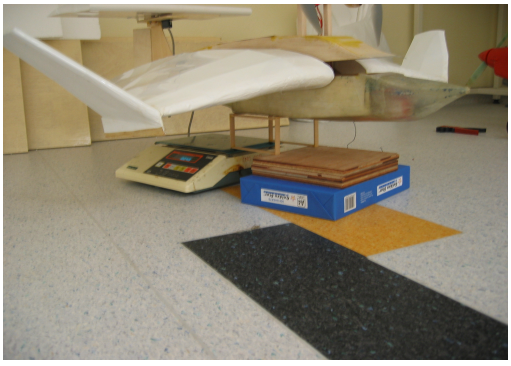

Figure 16: Illustration of the Experimental Setup

Table 2: Readings from weighing machine for calculating Y-Coordinate

R_1 /kg	R_2 /kg	R_3 /kg	R_{Avg} /kg	R_{FX} /N
0.048	0.050	0.047	0.049	***0.48***

Sample calculation:

Knowing that R_{FX} = **0.48N**, X_{CG} can be determined by taking moment about point A:

Taking anticlockwise moment as +ve:

$\Sigma M_A = - w (9.81) (0.135 – X_{CG}) + R_{FX} (0.135) = 0$

$- (2.027) (9.81) (0.135 - X_{CG}) + (0.48) (0.135) = 0$

X_{CG} = 0.132m (from the step of the hull)

Note that: this is equivalent to **0.15m from the leading edge** of the wings

Z-Coordinate:

The experimental setup for finding the Z-Coordinate of the CG position is shown in the following diagram and the table records the readings obtained:

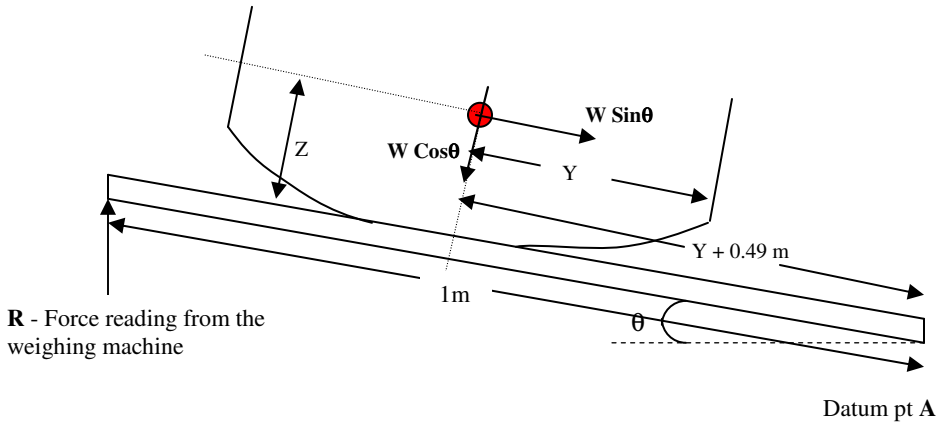

Figure 17: Free Body Diagram

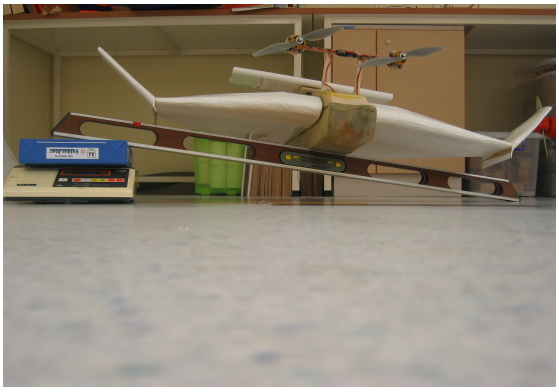

Figure 18: Illustration of the Experimental Setup

Table 3: Readings from weighing machine for calculating Z-Coordinate

θ / °	R_1 /kg	R_2 /kg	R_3 /kg	R_{Avg} /kg	R_{FZ} /N
5	1.090	1.060	1.105	1.085	***10.64***
8	1.060	1.020	1.040	1.040	***10.20***
10	1.015	1.045	1.027	1.029	***10.09***

Sample calculation:

For **θ = 5°:** Knowing that R_{FZ} = **10.64N** and **Y_{CG} = 0.050m**, Z_{CG} can be determined by taking moment about point A:

Taking anticlockwise moment as +ve:

$\Sigma M_A = w\,(9.81)\,(\text{Cos}\theta)(Y_{CG} + 0.49) - R_{FZ}\,(1)(\text{Cos}\theta) - w(9.81)(\text{Sin}\theta)(Z_{CG}) = 0$

$(2.027)\,(9.81)\,(\text{Cos } 5)(0.05 + 0.49) - (10.64)\,(\text{Cos } 5) - (2.027)(9.81)(\text{Sin } 5)\,(Z_{CG}) = 0$

Z_{CG} = 0.111m (from the lowest point of the hull)

4.4 Thrust Line Alignment

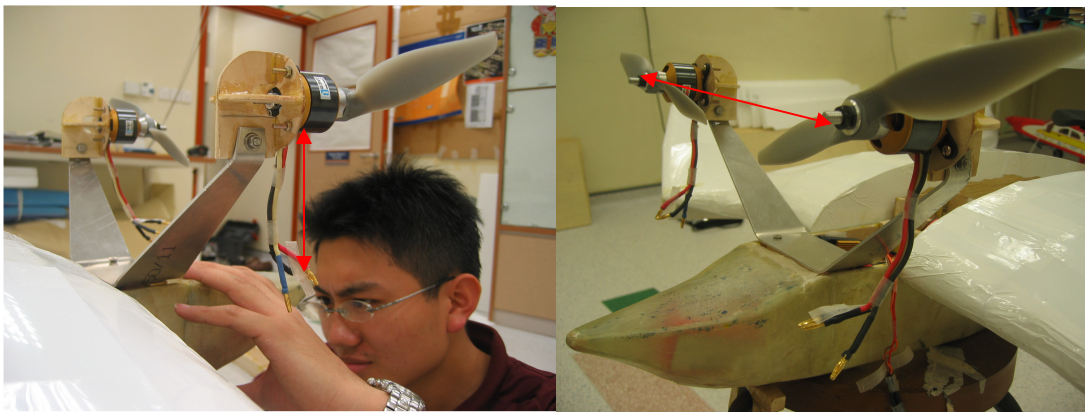

Figure 19: Measurements taken to ensure vertical and horizontal alignment of the motors

Another important aspect that is to be taken into account is the alignment of the thrust line. Since the WIG Craft is propelled by 2 engines, it is imperative to ensure that the 2 engines are inline, horizontally and vertically, with respect to each other (refer to Figure 19). Any misalignment is likely to cause the aircraft to exhibit tendencies to drift, yaw or even roll over when the motors are throttled up. This will create an inherent turning moment, which causes instability and prevents the aircraft from gathering sufficient straight line speed required during take off.

In addition, the motors must be mounted at equal distances from the centre line to ensure that there is no tendency to yaw. The sides of the fuselage and the centre line are chosen as 3 datum points from which the motors' thrust lines can be determined with reasonable accuracy. Three laser pointers are used in a simple experiment to determine whether the 2 motors are at equidistance from

the centre line. With the help of a simple jig, one of the laser pointers is referenced with the center line of the aircraft, while the other 2 are adjusted until they are aligned with the 2 motor shafts, as shown below:

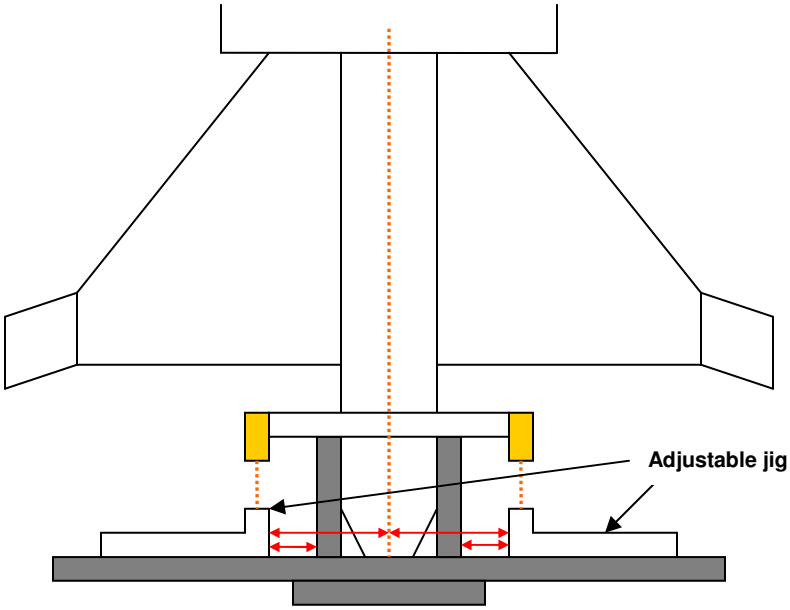

Figure 20: Experimental setup for the alignment of the motor shafts

With the aid of this experiment, it reduced the error in the mounting positions of the two motors to approximately 0.5mm. Condition for accuracy is achieved when both laser spots coincide with the respective motor shaft and the distance from the center line to each motor shaft does not differ by more than ±1mm.

5 Aerodynamics Control of WIG Aircraft

Aerodynamics control refers to the ability of the aircraft to respond to changes in motion parameters when controls are activated. A complete control system will typically include the control surfaces, electronic servos, receiver, control and servo horns and connecting rods.

5.1 Design of Control Surfaces and Analysis of Their Effectiveness

An integral part of implementing the flight control system is the designing of control surfaces. In this model WIG aircraft, design considerations are made for an elevator, for pitch (longitudinal) control; and a rudder, for yaw (directional) control.

5.1.1 Elevator

When the elevator is deflected, it changes the lift and pitching moment of the aircraft, and these changes can be expressed as:

$\Delta C_L = C_{L\delta e}\delta_e \qquad \Delta C_M = C_{M\delta e}\delta_e$

Therefore, in evaluating the effectiveness of the elevator, the two important parameters to consider are $C_{L\delta e}$ and $C_{M\delta e.}$ They are related to the aerodynamics and geometric characteristics of the horizontal tail in the following manner:

$$C_{L\delta e} = S_t/S\ \eta(dC_{Lt}/d\delta_e) = S_t/S\ \eta(dC_{Lt}/d\alpha_t)\ (d\alpha_t/d\delta_e) = S_t/S\ \eta C_{L\alpha t}\ \tau \qquad (17)$$

where τ is the flap effectiveness parameter and is obtained from existing aerodynamics data graph (from reference [1] page 64), using the ratio of control surface area to lifting surface area.

Knowing $\mathbf{C_{L\alpha t}} = \mathbf{0.0578}$ /° and $\tau \approx \mathbf{0.15}$, it can calculated that

$\mathbf{C_{L\delta e}} = (0.140/\ 0.25)\ (1)\ (0.0578)\ (0.15) = \mathbf{0.0049}$ /°

Similarly,

$$C_{M\delta e} = -V_H \eta (dC_{Lt} / d\delta_e) = -V_H \eta (dC_{Lt} / d\alpha_t)(d\alpha_t / d\delta_e) = -V_H \eta C_{L\alpha t} \tau \qquad (18)$$

$\mathbf{C_{M\delta e}}$ = - 0.488 (1) (0.0578) (0.15) = **- 0.0042** /°

To verify the above theoretical calculations on the effectiveness parameters of the elevator design, a series of CFD simulations are done on the horizontal tail stabilizer unit to calculate the change in forces and moments acting on the tail when the elevator is deflected. The diagram below shows an example of the static pressure contour plot obtained from CFD.

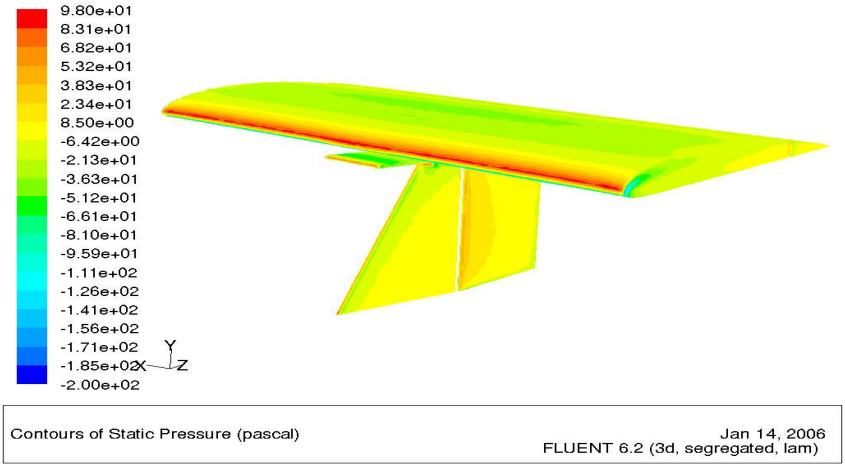

Figure 21: CFD static pressure contour plot of the horizontal tail stabilizer

Analysing the lift and moment readings obtained from simulation, it is found that $\mathbf{C_{L\delta e}}$ **= 0.0048** /° and $\mathbf{C_{M\delta e}}$ **= - 0.0038** /°, which are both close to the theoretical values obtained above.

5.1.2 Rudder

By rotating the rudder, the lift force (which in this case is the side force) on the vertical surface is varied to create a yawing moment about the C.G of the aircraft. The rudder control effectiveness is thus defined as the rate of change of yawing moment with respect to rudder deflection angle and is given by:

$C_{n\delta r} = - \eta(l_v S_v / Sb) (dC_{Lv}/d\delta_r) = - \eta V_v (dC_{Lv}/d\alpha_v) (d\alpha_v/d\delta_r) = - \eta V_v C_{L\alpha v} \tau$ (19)

Knowing that $\mathbf{C_{L\alpha v} = 1.704}$ /° and $\mathbf{\tau = 0.8}$

$\mathbf{C_{n\delta r}}$ = - (1) [(0.535 x 0.018) / (0.25 x 0.93)] (1.704) (0.8) = **- 0.0565** /°

Similarly, to verify the effectiveness of the rudder, a series of CFD simulations are done to find out the change in forces and moments acting on the rudder when it is deflected. This will help determine the directional control on the aircraft.

Analysing the moment readings obtained from simulation, it is found that $\mathbf{C_{n\delta r}}$ = **- 0.0523** /°, which is again very close to the theoretical value obtained above.

5.2 Selection of Control Electronics

The process of selecting appropriate servos, for the respective control surfaces, is aided through CFD simulations. The main consideration is that the servo must be able to provide the necessary torque to deflect the control surface through the required angle range. By modeling the control surfaces under ideal flight conditions and deflecting them at various angles, a series of simulations are done to compute the change in force and moment generated about the hinge. This is to determine the load torque acting on the respective control surfaces at various angle of deflection, and will help to determine the moment specifications required on the servos controlling the surfaces.

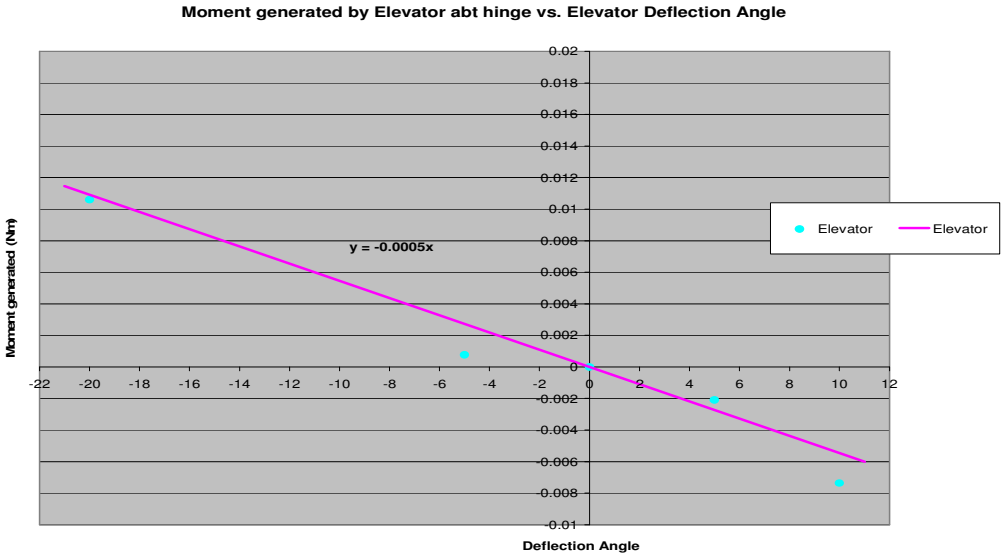

Figure 22: Graph of moment generated about the hinge against angle of deflection

From Figure 22 above, the maximum torque required to deflect the elevator, under ideal flying condition, through the angle range of -15 ° to 15 ° is about 0.08Nm.

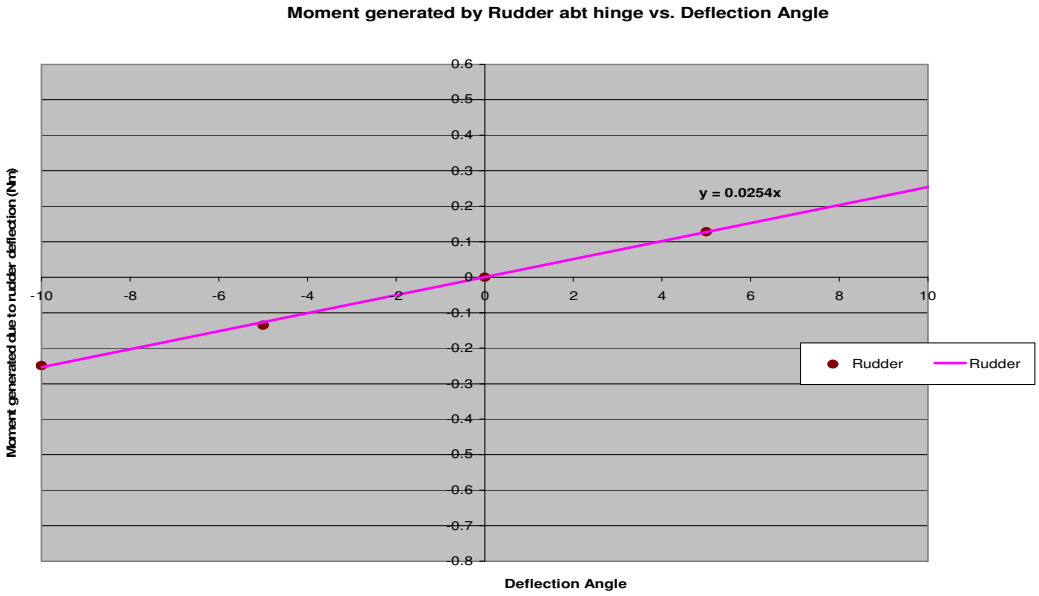

Figure 23: Graph of moment generated by rudder against angle of deflection

Similarly, from Figure 23 above, the maximum torque required to deflect the rudder through the angle range of -10 ° to 10 ° is about 0.25Nm.

Looking at both requirements and factoring in a safety factor of 20%, the servo must be able to provide a torque of approximately 0.30Nm. Table below shows a

series of servos that satisfy this torque requirement, and are thus shortlisted for selection consideration.

Table 4: Servo ratings and specifications

Model	Torque rating (Kg /cm)	Maximum Torque (Nm)	Weight (g)	Torque / weight ratio (Nm /g)
Hitec HS 81	3.0	0.294	16.6	0.0177
Hlitec HS 85	3.5	0.343	19.2	0.0179
Futaba S3102	3.7	0.363	21	0.0173
Futaba S3003	4.1	0.402	48.2	0.00834
Futaba S148	4.1	0.402	45.4	0.00886

As weight is an important design factor in constructing the WIG aircraft, torque to weight ratio is used as the selection parameter. As seen in table above, **HITEC HS 85 servo** offers a torque to weight ratio of 0.0179Nm/g and is the best among the several models considered. The detail specifications of this selected servo are attached in Appendix B.

5.3 Determining the Servo Characteristics

To determine the transfer function and understand the characteristic of the selected servo, an experiment is designed and setup, as illustrated below:

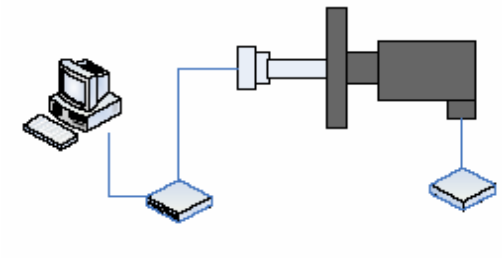

Figure 24: Schematic of the experimental setup

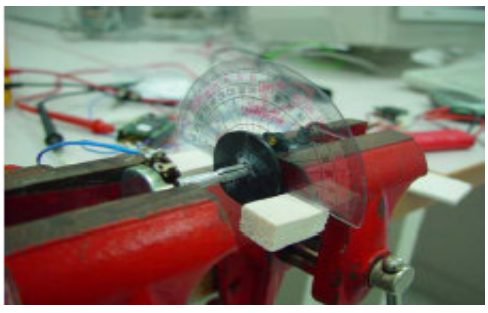

Figure 25: Servo deflection measurement

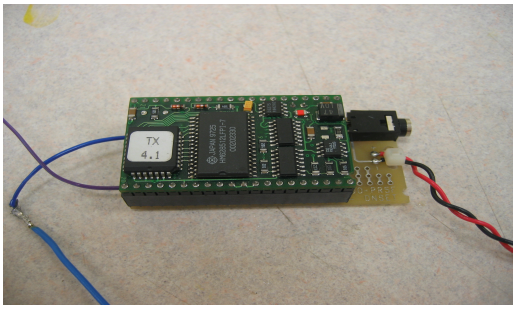

Figure 26: Tattletale data logger

The objective of this experiment is to study the time response of the output of the servo under a unit step input signal. The Tattletale 5F data logger is programmed in TXBASIC language and the sampling interval is set at 10ms, to provide an accurate transient response of the HS 85 servo. The TXBASIC program used is shown in Appendix D.

In this experiment, the receiver will receive a step input from the transmitter and send it to the servo. The output response will be detected and recorded by the data logger. The transient unit step response of the servo is then obtained by plotting output readings against time, as soon in Figure 27 below:

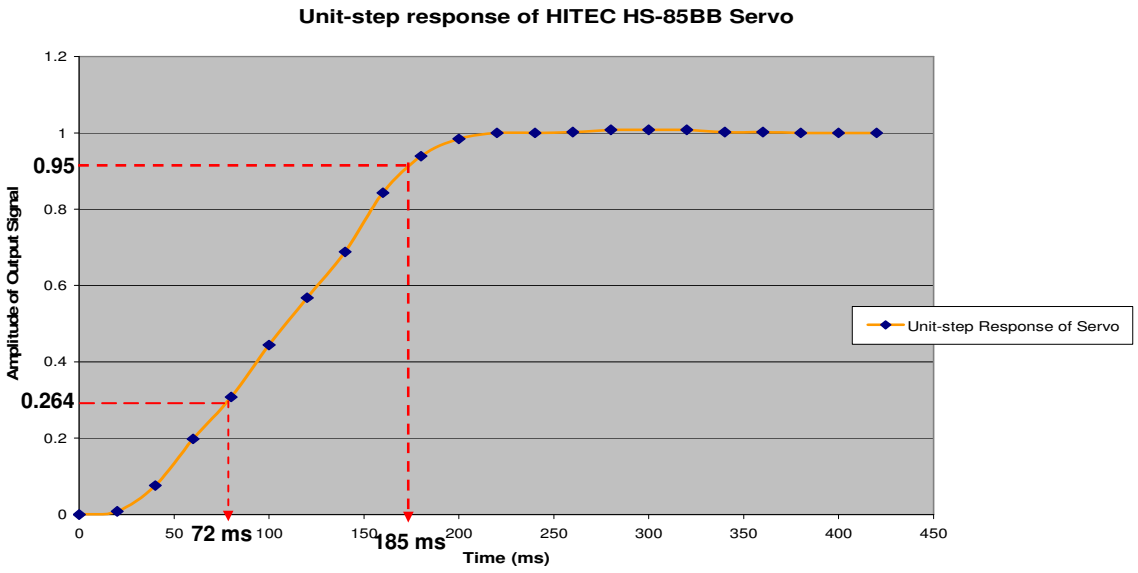

Figure 27: Graph of output signal of servo against time

By modelling the HS 85 servo system as a critically damped 2nd order system **(ζ=1)** with no overshoot **(M_p=0)**, the transfer function of the servo and its system characteristic can be obtained from the graph.

For 2nd order system, the transfer function can be generally expressed as:

$$\frac{C(s)}{R(s)} = \frac{\omega_n{}^2}{s^2 + 2\varsigma\omega_n s + \omega_n{}^2} = \frac{\omega_n{}^2}{(s+\omega_n)^2}$$

Given a unit step input $\left(\frac{1}{s}\right)$ and taking inverse Laplace Transform, the output response can be mathematically expressed as:

$$c(t) = 1 - e^{-\omega_n t}(1 + \omega_n t) \qquad (20)$$

From equation (20), when $t=1/\omega_n$ (time constant), c(t) =1 – 0.736 = 0.264. Therefore, $\omega_n = 1/t_{0.264} = 13.90$. Furthermore, from the graph, it can be observed that Rise time, t_r, which is defined as the time taken for the output response to rise from 5% to 95% of its final value, is **0.150s**. Similarly, Settling time, t_s, which is the time required for the response curve to reach and stay within a 2% range about the final value, is **0.200s**.

5.4 Integration of Control System

The integration of the various control components is done using mechanical connection joints: control horns, servo horns and connecting rods. The servos are connected to the receiver, using standard gauge wires, at dedicated channels. Suitable locations for each of the components are carefully chosen, when fixing them on board the model aircraft. Considerations taken in this process include the overall CG of the aircraft, ease of assembly and the structural limitations. Figure 28 below illustrates how the entire control system looks like when it is connected and fixed on board.

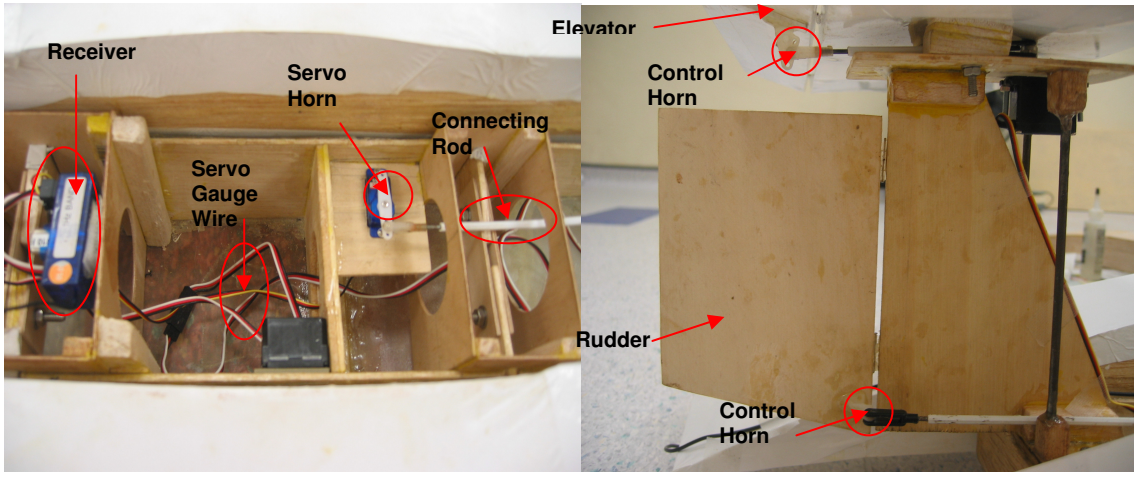

Figure 28: Control components and their connecting parts

6 Designing the Automatic Height Control System

One of the objectives in this project is to implement an automatic height control system capable of sustaining the model WIG aircraft at the ideal flying altitude, so that the required L/D ratio and a stable flight motion are achieved. The basic concept adopted is that during the initial take off, the pilot can remotely switch on this system, which will take over the control of the elevator and correct the flying altitude until the ideal level is reached and maintain it there. In addition, this system can also be used to provide accurate flight altitude data. The whole system will require various hardware components, written algorithm control logic and the understanding of the flight motion dynamics and transfer functions.

A schematic diagram of the overall height control system is as follows:

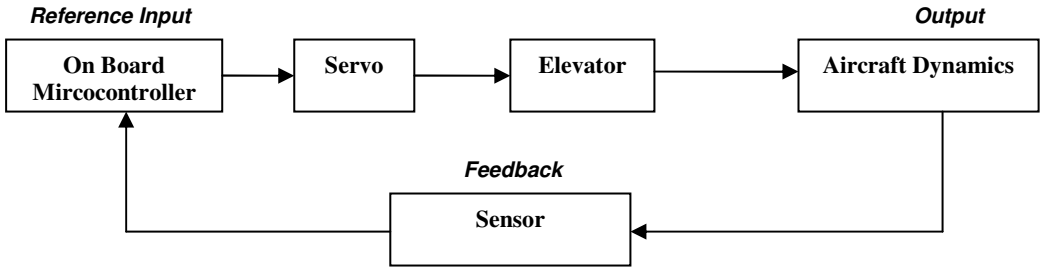

Figure 29: Schematic diagram of the control system

6.1 Hardware Selection and Testing

Hardware selection involves the consideration of important factors such as performance, reliability, weight, compatibility, availability, ease of use and cost. All selected hardware must then be tested, both independently and together as an integrated system, for their functionability under various conditions.

6.1.1 Microcontroller and Development Board

An integral hardware component in this automatic height control system is the on-board microcontroller, which is used to store the algorithm logic, receive

signals, store data and send out control commands to the actuator. In selecting this microcontroller, important factors of consideration includes: power consumption, processing speed, compatibility with other electronics, weight and cost. After careful consideration, **Parallax's BASIC Stamp 2SX (BS2SX-IC)** module is selected for this application. The microcontroller is somewhat like a single board computer, as it has its own processor, memory, clock, and interface (via 16 I/O pins). It serves as the 'brains' inside electronics applications, and is able to control and monitor switches, timers, motors, sensors, relays etc. Programming is performed using the PBASIC language. BS2SX-IC shows improved speed, larger program memory, faster serial I/O and higher resolution for time sensitive command when compared with many other available models. Furthermore, it comes with serial PC interface, which provides enhanced debug features, via an in-house editing software.

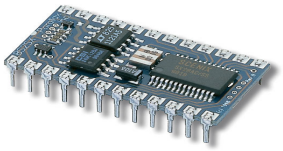

Figure 30: Parallax BASIC Stamp 2SX

In addition, this microcontroller also comes with a **BASIC Stamp II BOE Carrier Board**, which has a 24-pin DIP socket, specially designed to fit the controller. The carrier board allows for easy integration with other control components and the downloading of the programming codes. It serves as an ideal development platform for various control applications. For more details on the technical specifications of BS2SX-IC, the BOE Carrier Board and their respective schematic drawings, kindly refer to Appendix C

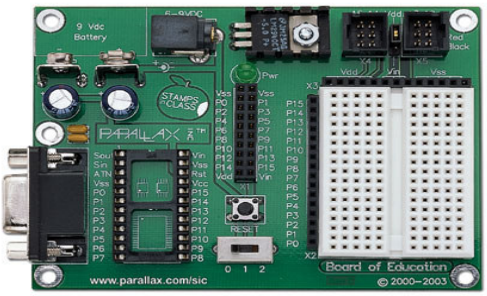

Figure 31: BASIC Stamp Board of Education development board

Finally, miscellaneous hardware requirements include a **6 – 9V DC battery jack**, which serves as the power source, and a **USB to Serial Adapter** to connect the microcontroller to a PC or laptop for programming and troubleshooting functions.

The various hardware components are then interconnected and tested with the servo to ensure compatibility, and verify that the microcontroller is able to send precise signal pulses to the servo at regular interval. Different signal pulse widths will result in the servo turning at different angles. As such, the objective here is to calibrate the servo and obtain this relationship between pulse width and servo deflection angle. This is to ensure that the microcontroller is able to control and turn the servo precisely through the angle range required. The amplitude, width and frequency readings of the pulses are obtained using an oscilloscope. A sample of the program used in this experiment and the calibration data collected are shown in Appendix E and the pictures below illustrate the experimental setup.

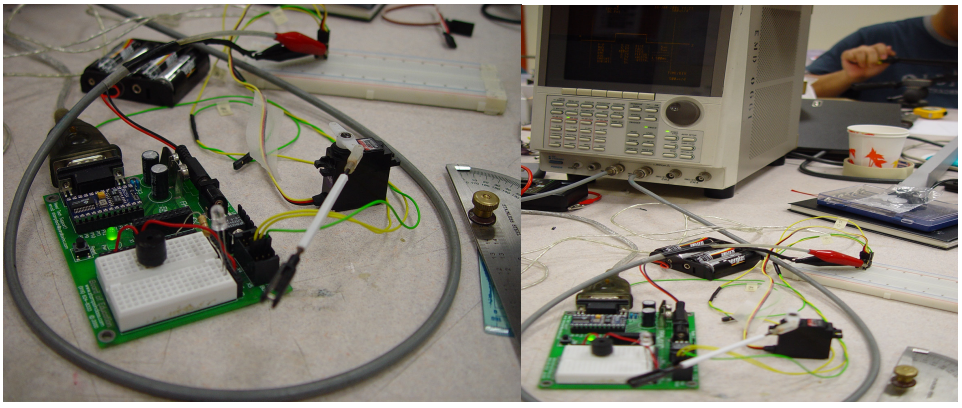

Figure 32 : Integrating the microcontroller with the servo to test for signals

6.1.2 Sensors

A sensor has to be implemented to provide accurate altitude measurements and feedback to the control loop. As the WIG aircraft is designed to fly at low altitude, between 5 to 25cm, and at speed of approximately 12 to 15m/s, the sensor chosen must have a sensing range capable of operating within this altitude and speed limits, and a blind zone of less than 5cm. In addition, the sensor must be able to function accurately over both hard ground and water surface, and must be compatible with the other hardware components. After considering several

sensors, operating under different principles such as capacitive, photoelectric and ultrasonic mode; as well as sensors with different scan techniques such as thru-beam, retro-reflective and diffuse scan, the **Parallax PING ultrasonic range finder - SRF08** is ultimately chosen. The sensor detects objects by emitting a 40kHz short ultrasonic burst and then "listening" for the echo. It has a sensing range of between 3 cm to 3.3m and as such, provides good coverage for the distance required. In addition, the PING sensor is designed by the same company that develops the BASIC Stamp microcontroller and as such, offers good hardware compatibility and easy integration.

Figure 33: PING ultrasonic sensor SRF08

Attached in Appendix C are some details involving the important features, theory of operation and test data of this sensor.

A simple experiment is also designed to verify that the sensor is able to take multiple readings, over both ground and water surface, and ensure its accuracy. The setup shown below explains how the sensor is tested to take readings over water surface at different height and across varying forward velocity.

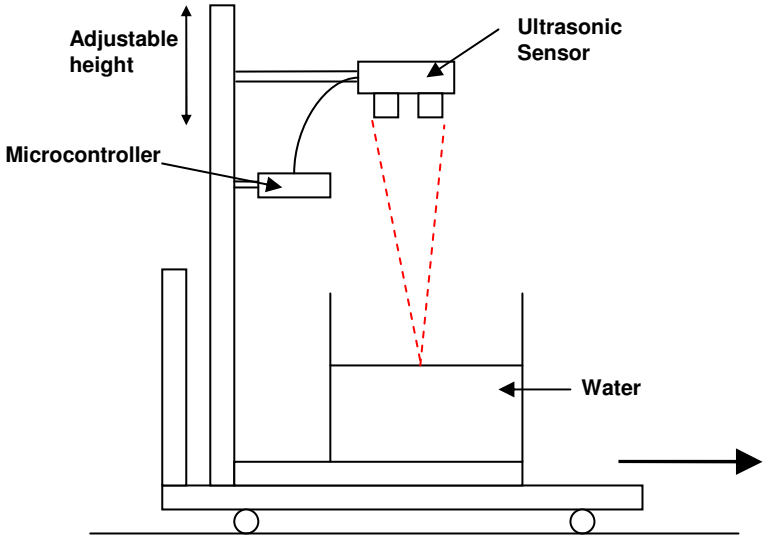

Figure 34 : Experimental setup for testing the sensor

6.2 Software Coding

All programs are written in PBASIC programming language using the BAISC Stamp Editor software v2.2. This software allows user to write and troubleshoot programs on a PC or laptop, before downloading them into the BASIC stamp microcontroller using a data cable. Syntax and reference manual on how to get started with programming using PBASIC can be found at Parallax official website. The various programs written for this project are attached in Appendix E

6.3 Establishing the Aerodynamics Transfer Function

The basic logic of this automatic height control system is to control the angle of deflection of the elevator, in order to generate the required change in moment on the tail. This change in tail moment will result in a change in the angle of attack of the aircraft and in turn produce a change in the height, to compensate for any deviation from the ideal flying altitude, as stipulated by the control logic program. To accomplish this function, it requires the calculation of the transfer function that represents the aircraft dynamics.

To understand the motion dynamics of the WIG aircraft, it is important to first determine its moment of inertia about the C.G. Since the objective is to implement an automatic height control system, pitch angle is the most crucial parameter, and the focus is thus to determine the moment of inertia along the pitch axis (X-axis). To simplify the calculation, the entire aircraft is divided into 6 subassemblies, and each subassembly is then approximated to standard solid shapes. Details of the calculation are shown in Appendix F.

The total moment of inertia about the pitch axis, $\mathbf{I_{yy}}$ of the model WIG aircraft is calculated to be **0.183 kgm^2**.

Moment generated due to $\Delta\alpha$ = ΔLift on the tail x moment arm, l_t

$M(\alpha) = - l_t (\Delta Lift) = - l_t (C_{L\alpha t}\, \alpha\, Q\, S_t) = C_{M\alpha t}\, \alpha\, Q\, S_t$ (21)

Where $Q = 0.5\, \rho\, U^2$ and S_t is the area of the tail

Taking derivative with respect to α:

$dM/d\alpha = C_{M\alpha t} Q S_t$ (22)

Note that the change in angle of attack, $\Delta\alpha$ on an aft surface can be approximated using small angle approximation:

$\tan\Delta\alpha = q l_t/U$

Therefore for small angle, $\Delta\alpha \approx q l_t/U$

Now consider the moment contribution due to pitching velocity (pitch rate) q:

$M(q) = - l_t (C_{L\alpha t} \Delta\alpha Q S_t) = - l_t [C_{L\alpha t} (q l_t/U) Q S_t]$ (23)

Taking derivative with respect to q:

$dM/dq = - l_t [C_{L\alpha t} (l_t/U) Q S_t]$ (24)

The equation of motion governing the pitching motion can be derived as follows:

$M = I_{yy} \Delta\ddot{\alpha}$ (25)

Generally, pitching moment, M can also be expressed as a function of change in angle of attack, rate of change of angle of attack, change in pitch rate and change in elevator deflection as shown below:

$M = f(\Delta\alpha, \Delta\dot{\alpha}, \Delta q, \Delta\delta_e) = (dM/d\alpha) \Delta\alpha + (dM/d\dot{\alpha}) \Delta\dot{\alpha} + (dM/dq) \Delta q + (dM/d\delta_e) \Delta\delta_e$ (26)

Equating equation (25) and (26),

$\Delta\ddot{\alpha} - (M_q + M_{\dot{\alpha}}) \Delta\dot{\alpha} - M_\alpha \Delta\alpha = M_{\delta e} \Delta\delta_e$ (27)

where $M_q = (dM/dq)/ I_{yy}$ $M_{\dot{\alpha}} = (dM/d\dot{\alpha})/ I_{yy}$ $M_\alpha = (dM/d\alpha)/ I_{yy}$ $M_{\delta e} = (dM/d\delta_e)/ I_{yy}$

and $\Delta q = \Delta\dot{\alpha}$

Note that the moment contributions from the wings are neglected in the formulation of the above equation. This is because all moment calculations are taken with respect to the C.G position of the aircraft, which is very close to the aerodynamic centre of pitch of the wings and thus, the moment arm for the wings is very small, leading to negligible moment contributions.

Now taking Laplace Transform of equation (27),

$$s^2F(s) - sf(0) - \dot{f}(0) - (M_q + M_{\dot{\alpha}})(sF(s) - f(0)) - M_\alpha F(s) = M_{\delta_e}\Delta\delta_e \qquad (28)$$

Note that $f(0) = \dot{f}(0) = 0$. Also, the contribution due to $M_{\dot{\alpha}}$ in equation (28) is ignored because this term is primarily due to the interaction of the wing wake on an aft surface. This effect is negligible in this WIG aircraft configuration because the tail is mounted at a high vertical location such that it is exposed to little downwash.

Rearranging equation (28) yields:

$$F(s)\left[s^2 - M_q s - M_\alpha\right] = M_{\delta_e}\Delta\delta_e$$

$$\Delta\alpha(s)\left[s^2 - M_q s - M_\alpha\right] = M_{\delta_e}\Delta\delta_e$$

$$\frac{\Delta\alpha(s)}{\Delta\delta_e} = \frac{M_{\delta_e}}{s^2 - M_q s - M_\alpha} \qquad (29)$$

Let the change in height due to the pitching moment be Δh.

For small angle, V ≈ U

$$\Delta\dot{h} = V\sin(\Delta\alpha) = U\Delta\alpha \qquad (30)$$

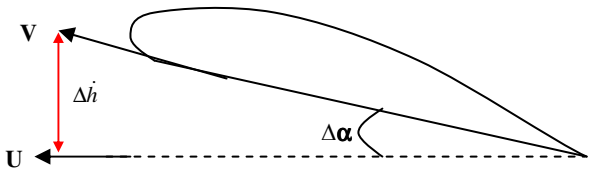

Now taking Laplace Transform of equation (30),

$$s\Delta h(s) = U\Delta\alpha(s)$$

Dividing by $\Delta\delta_e$ throughout, the transfer function becomes:

$$\frac{\Delta h(s)}{\Delta\delta_e} = \frac{U}{s}\frac{\Delta\alpha(s)}{\Delta\delta_e} = \frac{U}{s}\left(\frac{M_{\delta_e}}{s^2 - M_q s - M_\alpha}\right) \qquad (31)$$

From earlier results and corresponding graphs,

- **$C_{M\alpha t}$ = - 0.0273** /°
- **$C_{L\alpha t}$ = 0.0578** /°
- **$M_{\delta e}$ = 0.0162** /°

- S_t = **0.140 m²**
- I_{yy} = **0.183 kgm²**

From equation (22) and (27),

$\mathbf{M_\alpha} = C_{M\alpha t}\, Q\, S_t / I_{yy} = (-0.0273)(0.5 \times 1.2 \times 12^2)(0.140)/0.183 =$ **-1.824 /s²**

From equation (24) and (27),

$\mathbf{M_q} = -\, l_t\, [C_{L\alpha t}\, (l_t/U) Q\, S_t] / I_{yy}$

$= -(0.465)(0.0578)(0.465/12)(0.5 \times 1.2 \times 12^2)(0.140)/0.183 =$ **-0.0696 /s**

Therefore the transfer function of the aircraft dynamics is:

$$\frac{\Delta h(s)}{\Delta \delta_e} = \frac{12}{s}\left[\frac{0.0162}{s^2 + 0.0696s + 1.824}\right] = \left[\frac{0.1944}{s^3 + 0.0696s^2 + 1.824s}\right]$$

This represents a 3rd order system. Assuming a unit step input $\left(\frac{1}{s}\right)$ and taking inverse Laplace Transform:

Output signal, $\Delta h(t) = L^{-1}\left(\frac{1}{s}\left[\frac{0.1944}{s^3 + 0.0696s^2 + 1.824s}\right]\right)$

$$= 0.1066t - 0.0041 + 0.0041e^{-0.0348t}\cos(1.35t) - 0.079e^{-0.0348t}\sin(1.35t)$$

6.4 Overall Transfer Function of the System

Figure 35 below shows the block diagram of the automatic height control system

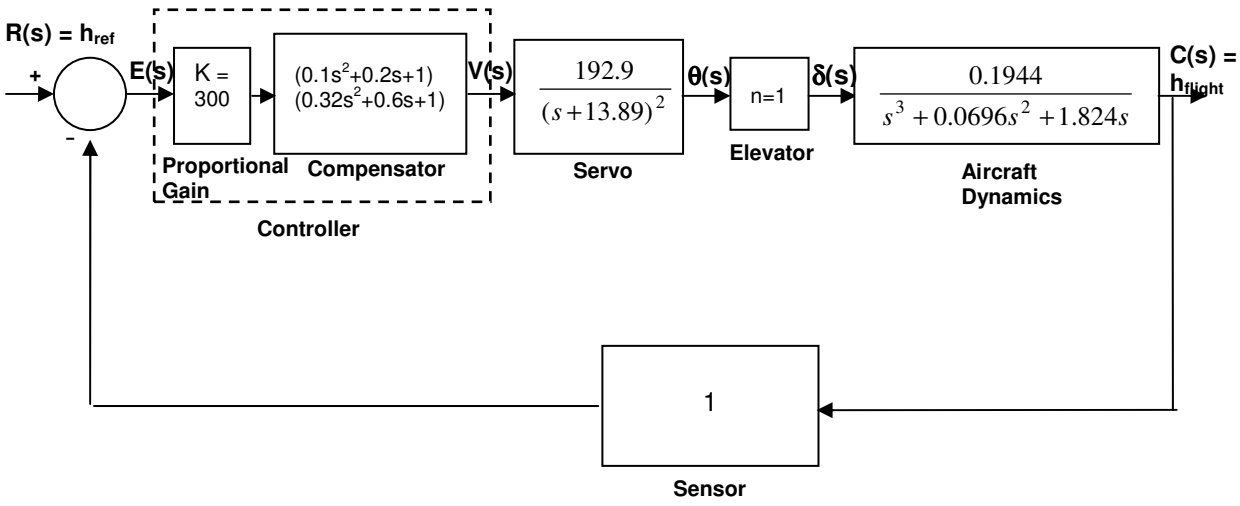

Figure 35 : Block diagram representation of automatic height control system

Notice that a proportional control, with a 4th order compensator, is implemented in this system. The gain value, K, which is set at 300 for this model, can be adjusted accordingly to obtain the ideal output response graph, with the desired rise time, settling time and within the maximum percentage overshoot allowed.

A system is Bounded-input Bounded-output (BIBO) stable if whenever the input signal r(t) is bounded, so is the output signal c(t). To verify the absolute stability of this system and ensure that the output signal is bounded, Routh's Stability Criterion is used. This analysis technique helps to determine whether all the roots in the characteristic equation of the closed loop transfer function have negative real parts and thus, lie in the open left half of the s-plane. This forms the essential condition for BIBO system stability.

Considering the 5th order polynomial characteristic equation,

$$\mathbf{s^5 + 39.37s^4 + 489.16s^3 + 2678.6s^2 + 9351.85s + 11250}$$

The Routh table is as follows:

s^5	1	489.16	9351.85
s^4	39.37	2678.6	11250
s^3	421.12	9066.1	0
s^2	1831.02	11250	
s^1	6478.69	0	
s^0	11250		

Routh's stability criterion states that the number of roots in the polynomial with positive real parts is equal to the number of sign changes in the coefficients of the first column of the array. Since there is no sign change observed, it can be concluded that all the roots in the characteristic equation of the closed-loop transfer function lie in the open left half s-plane, and the system enjoys absolute stability.

In addition, to investigate the relative stability of the system, Root Locus plot analysis is done using MATHLAB and the results are shown in Appendix G. The

analysis shows that the system's unit response has a rise and settling time of approximately 0.25 and1.5 sec respectively, and the system is stable.

6.5 Implementation of the System

After selecting the necessary hardware components, writing the control algorithm and determining the overall transfer function, the system is installed on board the model aircraft, ready for testing.

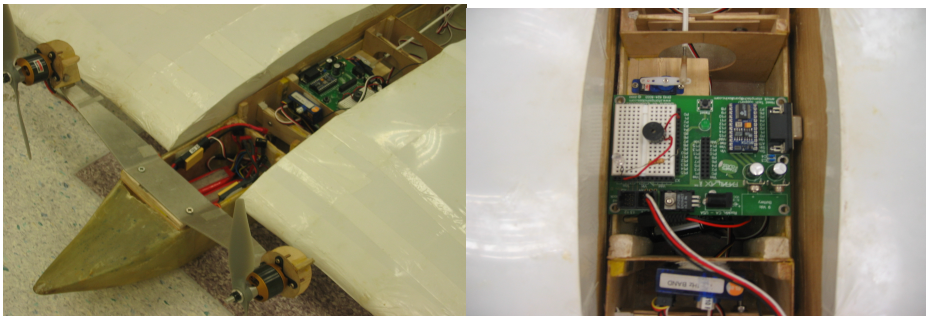

Figure 36 : Automatic height control system installed in the WIG aircraft

The first stage of testing the system involves a static test in the laboratory as shown in Figure 37 below.

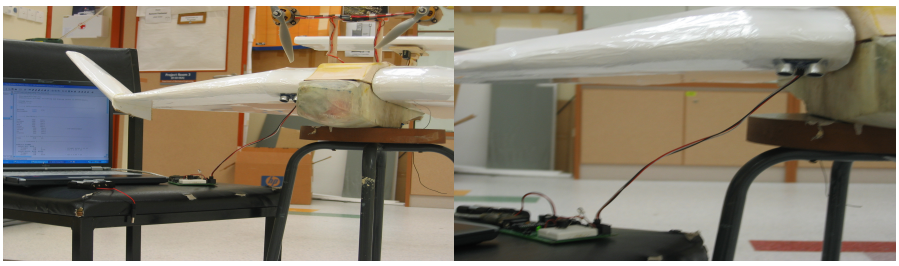

Figure 37 : Static test on the automatic height control system

The sensor is attached to the underside of the inverted delta wing and height readings are taken at varying altitude to test for the range of the sensor and accuracy of the measurements. The deflection of the elevator is also monitored to ensure that the control logic is functioning properly. The results of this experiment show that the sensor is able to measure and provide accurate height readings over the range of 3 to 50 cm, and is very responsive to any sudden height changes. The corresponding response of the elevator deflection angle is also very fast and precise. As such, it is concluded that the static performance of the height control system is satisfactory.

7 Flight Tests and Performance Evaluation

Flight tests are conducted over both hard ground and water surface to verify the amphibious and ground effect characteristics of the WIG aircraft, and measure its flight performance. This will also help to prove the accuracy of earlier simulation results. The automatic height control system is also tested to verify its performance and effectiveness. Several videos are taken and it is evident that the aircraft is capable of achieving Ground Effect on both land and water.

7.1 Ground Testing

Numerous tests are done on different hard ground surfaces to verify the ground effect on the model WIG aircraft. Before each actual test flight, a control and ground manoeuvring test is done to ensure that the aircraft responds to the input control command effectively, and that there is no observable instability.

Figure 38 : Ground effect mode (Indoor hard ground testing)

Outdoor hard ground testing locations include SRC running track and soccer field. However, when testing outdoor, the aircraft is often subjected to varying wind and weather conditions. As such, the performance of the aircraft is found to be inconsistent and unpredictable. This made the job of controlling the aircraft, in response to changing flying conditions, extremely difficult and challenging. As such the outdoor test flights are often unsustainable at the ideal flight speed and altitude, while take off distance is also unpredictable. To improve on the flight performance, indoor testing is conducted at MPSH, to eliminate environmental variables. Given this enclosed and controlled environment, the flight test results showed significant improvements and performance evaluation parameters are obtained more accurately. The automatic height control system is also found to be effective in helping the aircraft attain the ideal flight height.

7.2 Testing on Water Surface

Flight tests over water surface are conducted at a 35m swimming pool. The various tests show that the aircraft is able to sail and maneuver freely, un-stick

itself from the water surface and take off after some distance. Performance parameters are once again evaluated. However, given external disturbances such as varying wind and wave conditions, the performance of the aircraft is less consistent and piloting the aircraft is also more difficult.

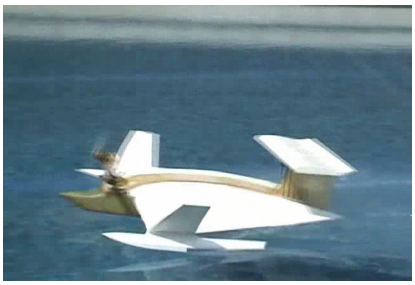

Figure 39 : Ground effect mode (Outdoor water testing)

7.3 Performance Evaluation Parameters

The main purpose of this section is to evaluate the performance of the WIG aircraft and compare the results with theoretical expectations. The performance parameters to be determined are: 1) Take off distance 2) Take off speed and 3) Cruising height

***Take off distance*:**

For the indoor hard ground testing, the take off distance is approximated by using the divider markings on the MPSH floor. Several flight tests are conducted and it is observed consistently that the aircraft starts to lift off the surface and get into the ground effect mode after travelling about the length of 3 dividers, which is approximately 20m. This take off distance is very much consistent throughout all the test flights conducted.

In measuring the take off distance in water test, aircraft's settings are kept constant, as per the hard ground test. Due to the increase in drag experience by the hull of the WIG aircraft, acceleration is affected, and thus the required take off distance increases accordingly. In addition, due to environmental variables, take off distance also varies quite substantially, from about 22m to 26m.

***Take off speed*:**

Take off speed is estimated by analysing video footages taken during test flight. For hard ground testing, the average take off speed is very consistent among all test flights and is approximately 10m/s. This is close to earlier theoretical speed estimation of about 12m/s required to lift the aircraft carrying the design payload.

For water testing, take off speed is approximately the same at about 10m/s, but a longer runway is required to achieve that speed.

***Cruising Height*:**

The automatic height control system is used to evaluate the cruising height of the aircraft. The on-board sensor is mounted under the wing, 5cm off the ground. The sensor readings for indoor hard ground testing, obtained at regular intervals of 0.5 sec, are plotted against flight time and shown in Figure 40 below.

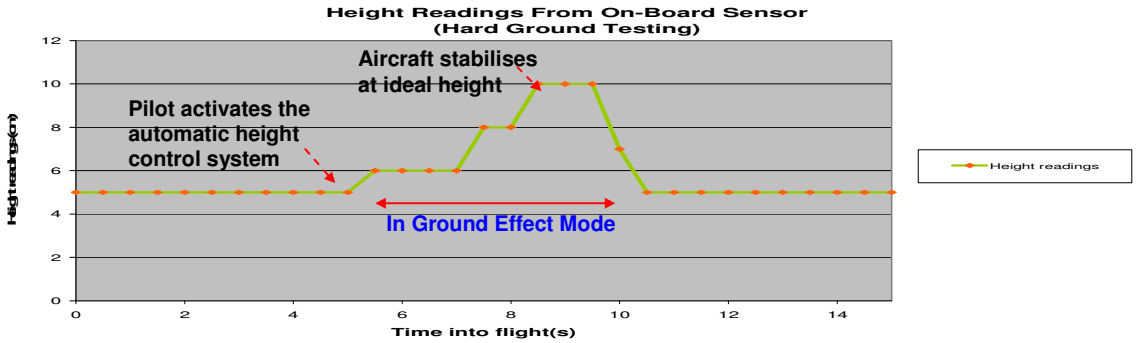

Figure 40 : Graph of height reading against time

Analysing the graph and looking at the different time periods:

- **0 – 3 sec:** Setting up the aircraft, checking the electronics and throttling the motor up to about 80% of its maximum speed.
- **3 – 5 sec:** The aircraft gradually gathers straight line speed, which is necessary to generate the required lift on the wings.
- **5 – 7 sec:** The aircraft begins gliding over the ground surface at about 1cm height, in a straight, forward motion. The automatic height control system is then enabled and takes over the control of the elevator.
- **7 – 8 sec:** The aircraft is lifted off the ground and is travelling at about 2 cm above ground surface.
- **8 – 10 sec:** The aircraft climbs gradually and stabilises at 5 cm off the ground. Notice that the aircraft attains this ideal flight height about 2 sec after activating the height control system. This is close to the theoretical settling time of 1.5 sec as predicted by the transfer function model earlier.
- **10 to 15 sec:** The height control system is disabled and the aircraft is landed as it approaches the end of the test ground. It comes to a complete stop about 2 sec after landing. The flight is not sustained any longer due to space limitation at the test ground.

The different time periods described above can be clearly seen from video footage taken. The automatic height control function is proven to be effective.

Similarly for water testing, altitude readings are shown in Figure 41 below.

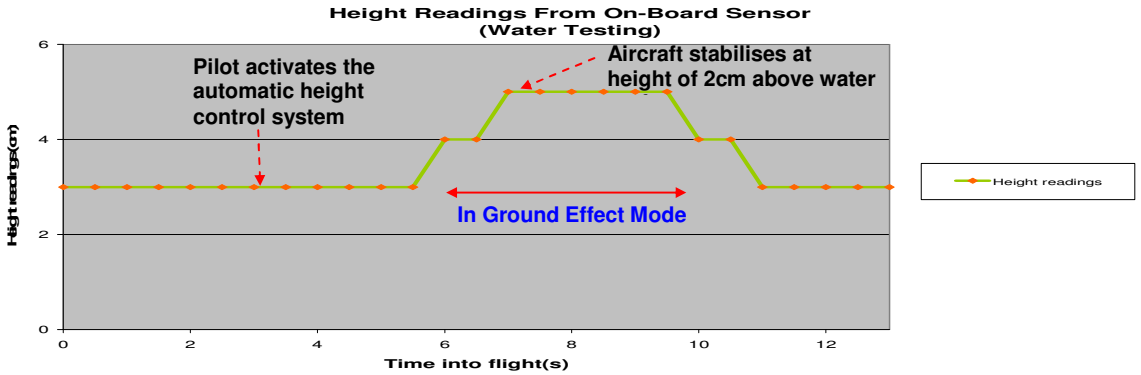

Figure 41 : Graph of height reading against time

Analysing the graph and looking at different time periods:

- **0 – 3 sec:** Setting up the aircraft, checking the electronics and throttling the motor up to its maximum speed.
- **3 – 6 sec:** The aircraft gradually gathers straight line speed, while the automatic height control system is enabled.
- **6 – 9 sec:** The aircraft is lifted off the water surface and climbs gradually to about 2 cm above the surface.
- **9 – 12 sec:** The height control system is disabled and the aircraft is landed. It comes to a complete stop almost immediately.

The effectiveness of the automatic height control function is not conclusive during the water test, as the aircraft is unable to attain the ideal flight height of 5cm from the surface. This is largely due to varying environmental conditions experienced during test flights, which creates unpredictable disturbance, and makes the controlling of the aircraft extremely difficult and challenging. External disturbances have not been modelled into the height control system and as such, the system is unable to response and compensate for such input. Furthermore, the height control system is modelled based on the assumption of the aircraft flying over hard ground, rather than water surface. As such, this might have contributed to the discrepancies observed.

8 Project Conclusion and Recommendations for Further Study

8.1 Project Conclusion

To fulfil the project objectives established at the start, it requires a multidisciplinary approach in engineering and design fundamentals. From the initial stage of designing and simulating 3-D model using computational software, to the fabrication of the aircraft, and finally implementing a control system and conducting numerous flight tests, all the various stages require careful consideration, testing and planning. The results obtained through simulations, experiments and theoretical calculations are compared against test flight performance and found to be reasonable and accurate. The stability and control aspect of an Inverted Delta WIG aircraft is thoroughly investigated. In summary, the achievements attained in this project include:

- Designing a workable WIG model aircraft, that is statically and dynamically stable in the ground effect regime.
- Designing a complete control system with automatic height control function, based on an understanding of the transfer function of the various control components and their time response characteristics.
- Demonstrating the effectiveness of using CFD and GAMBIT to perform a preliminary analysis on the WIG aircraft, and in designing the control surfaces and horizontal tail stabilizer unit.
- Fabricating and assembling the model aircraft, and conducting flight tests.
- Performing land and water-based take offs, and directional manoeuvres.
- Demonstrating the amphibious nature and speed of a WIG aircraft, which offer great potential in both military and commercial applications.

Lastly, this project has been enriching and extremely challenging, with many hands-on experiences that serve to further enhance and verify fundamental engineering concepts and theories learnt. The success of the project would never have been possible without the relentless effort of every team members.

8.2 Future Directions

With regards to this research area of ground effect on a small scale model aircraft, more studies and investigations can be made to enhance its performance. Recommendations for further research include:

- An in depth analysis of the hydrodynamics characteristic of the Inverted Delta WIG aircraft during the take off and landing mode,
- Designing an autopilot system that controls throttle speed and direction, allows compensation for external disturbances and can be integrated with the current automatic height control function,
- Implementing a collision avoidance system, so as to enhance the capability of the WIG aircraft to be used over various terrain, and
- Investigating the effect of undesirable sea states and varying wind and wave conditions on the performance and stability of the WIG aircraft.

List of References

1. Robert C. Nelson, “Flight Stability and Automatic Control”, 2nd edition McGraw Hill, 1998

2. Ogata K, “Modern Control Engineering”, Prentice Hall N.J, USA, 1997

3. Maskalik, D. Sinitsyn, “EKRANOPLANS Peculiarity of the theory and design”, St. Petersburg: Sudostroyeniye, 2000

4. Maskalik, D. Sinitsyn: “Amphistar First Civilian Ekranoplan”, St. Petersburg: Sudostroyeniye, 2000

5. H.H. Chun, C.H Chang, “Longitudinal Stability and Dynamic Motions of a small passenger WIG Craft”, Ocean Engineering 29, 2002, pp 1145-1162

6. Knud Benedict, Nikolai Kornev, Michael Meyer, Jost Ebert, “Complex mathematical model of the WIG motion including the take-off mode”, Ocean Engineering 29, 2002, pp 315-357

7. Nikolai Kornev, Konstantin Matveev, “Complex Numerical Modeling of Dynamics and Crashes of Wing-In-Ground Vehicles”,AIAA,2003-600, pp 1-9

8. Nocola de Divitiss, “Performance and Stability of a Winged Vehicle in Ground Effect”, Journal of Aircraft, Vol. 42, No. 1, 2005, pp 148-157

9. Staufenibel R. W., Schlichting U. J., “Stability of Airplanes in Ground Effect”, Journal of Aircraft, Vol. 25, No. 4, 1998, pp 289-294

Appendix A: Aerodynamic Coefficients Data and Graphs

The aerodynamic coefficients are obtained with the aid of CFD simulation software FLUENT and 3-D modelling software GAMBIT. The simulations are repeated for several angles of attack (AOA), under ideal flying height and velocity, and the readings obtained are plotted accordingly. The equations of the plotted graphs reveal important aerodynamic coefficients. The criteria for static stability, as stated in equation (1), (2), (3) and (6) are then analysed by processing the simulation results obtained, to determine the required parameters and coefficient derivatives.

For Wing Alone / Wing plus Hull Configuration:

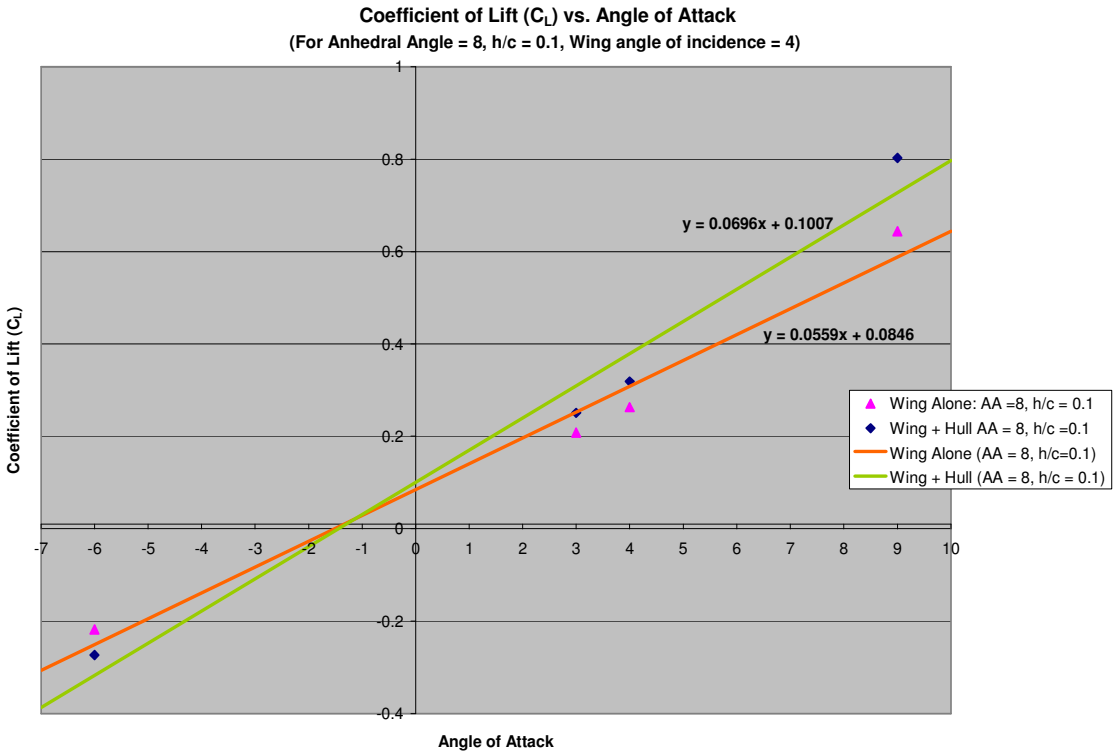

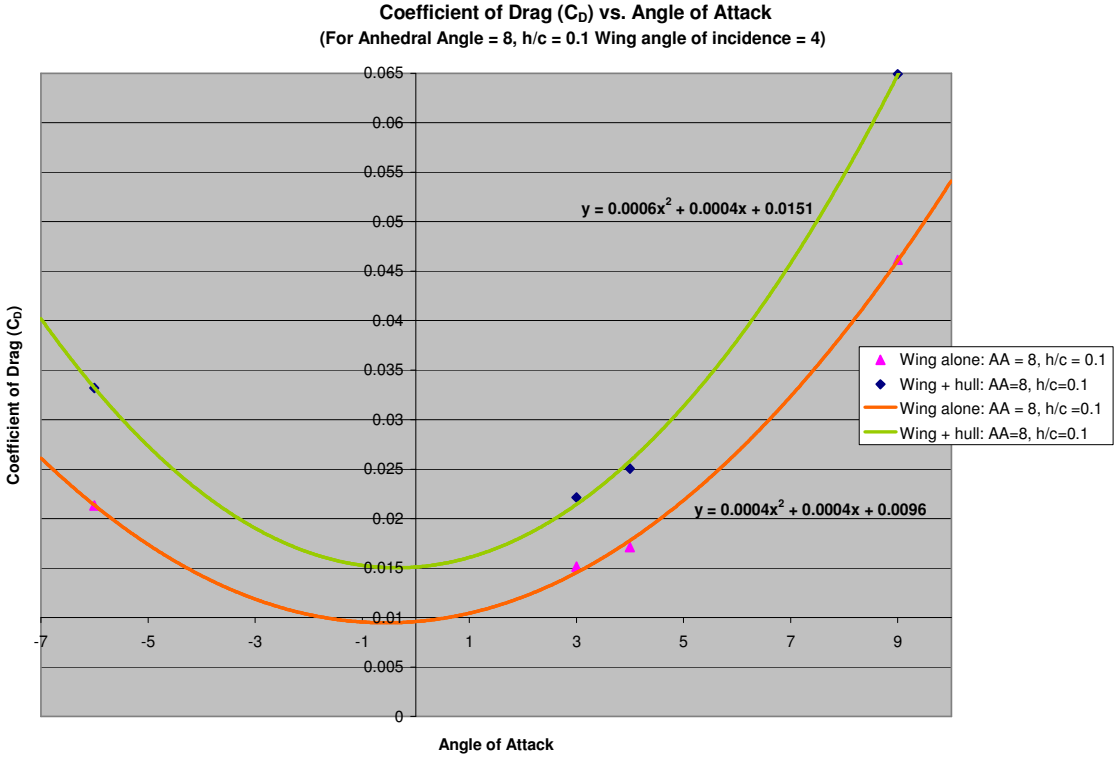
Coefficient of Drag (C_D) vs. Angle of Attack
(For Anhedral Angle = 8, h/c = 0.1 Wing angle of incidence = 4)
Coefficient of Drag (C_D)
Angle of Attack
y = 0.0006x² + 0.0004x + 0.0151
y = 0.0004x² + 0.0004x + 0.0096
Wing alone: AA = 8, h/c = 0.1
Wing + hull: AA=8, h/c=0.1
Wing alone: AA = 8, h/c =0.1
Wing + hull: AA=8, h/c=0.1

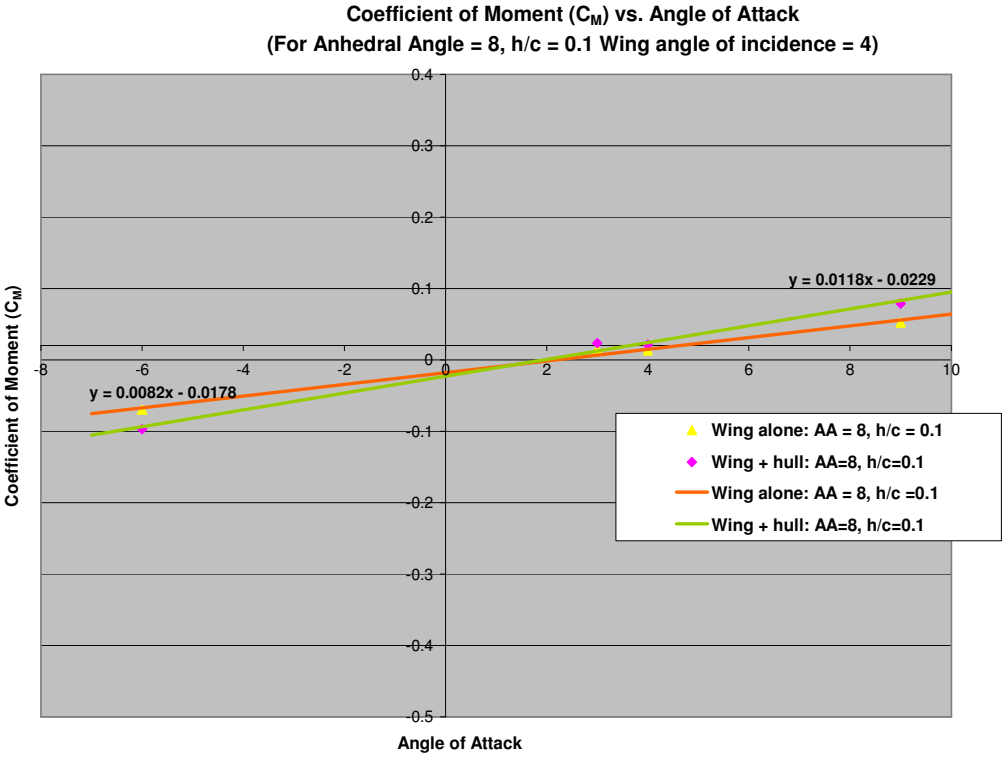
Coefficient of Moment (C_M) vs. Angle of Attack
(For Anhedral Angle = 8, h/c = 0.1 Wing angle of incidence = 4)
Coefficient of Moment (C_M)
Angle of Attack
y = 0.0118x - 0.0229
y = 0.0082x - 0.0178
Wing alone: AA = 8, h/c = 0.1
Wing + hull: AA=8, h/c=0.1
Wing alone: AA = 8, h/c =0.1
Wing + hull: AA=8, h/c=0.1

For Tail Alone Configuration:

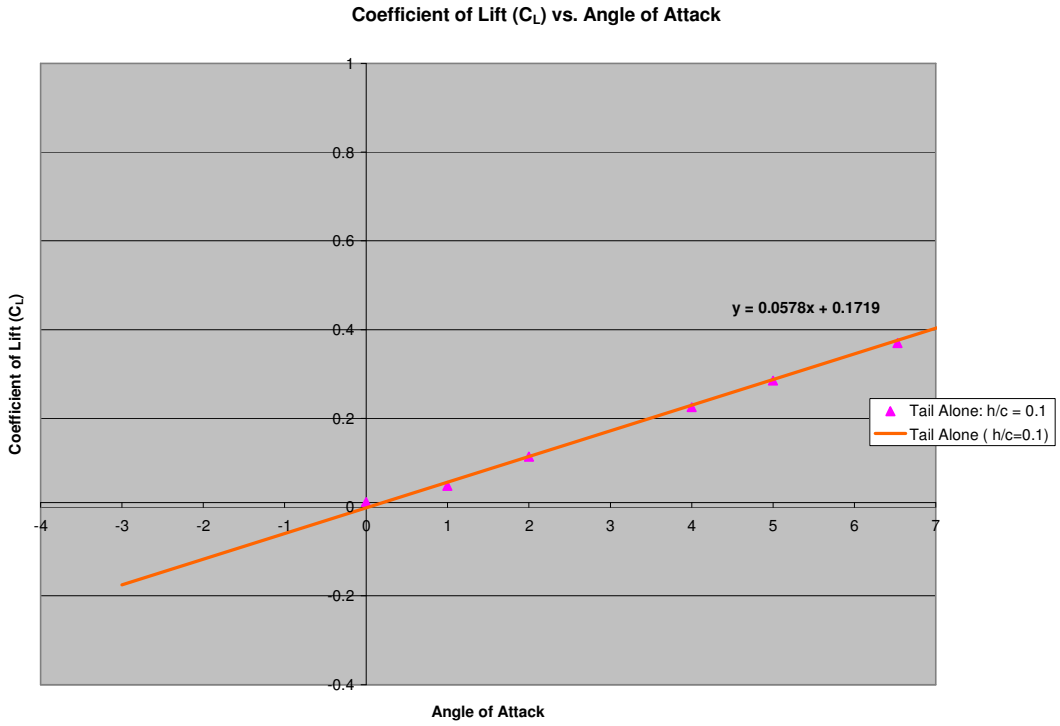

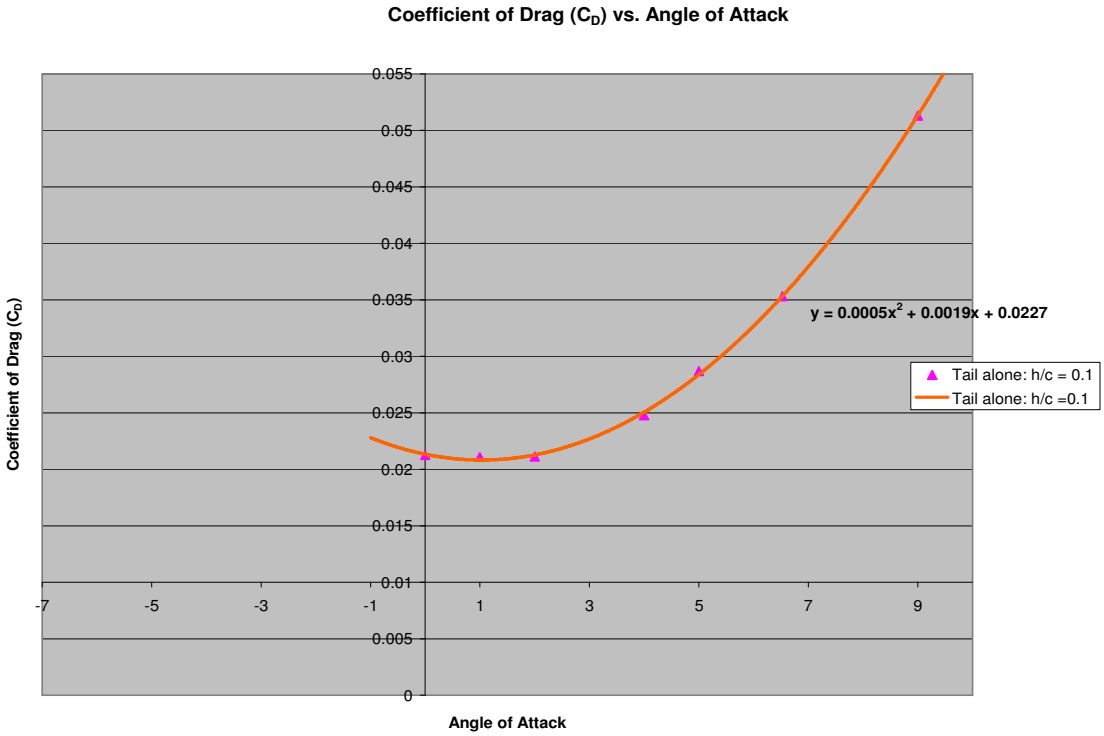

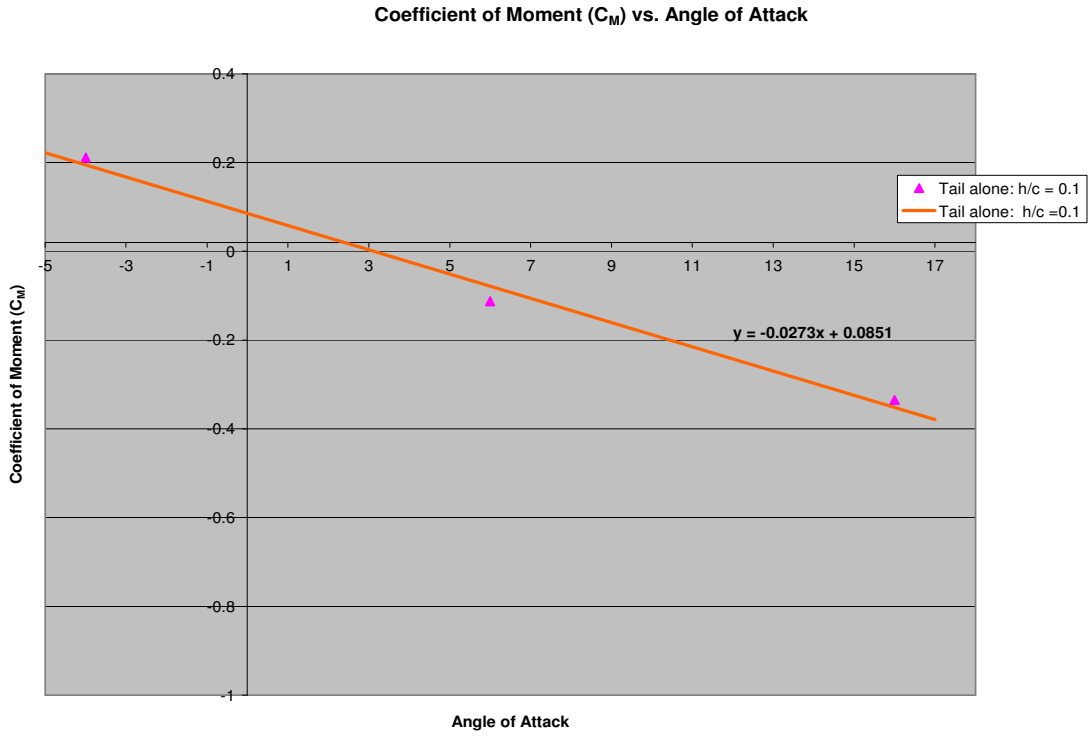

For Elevator:

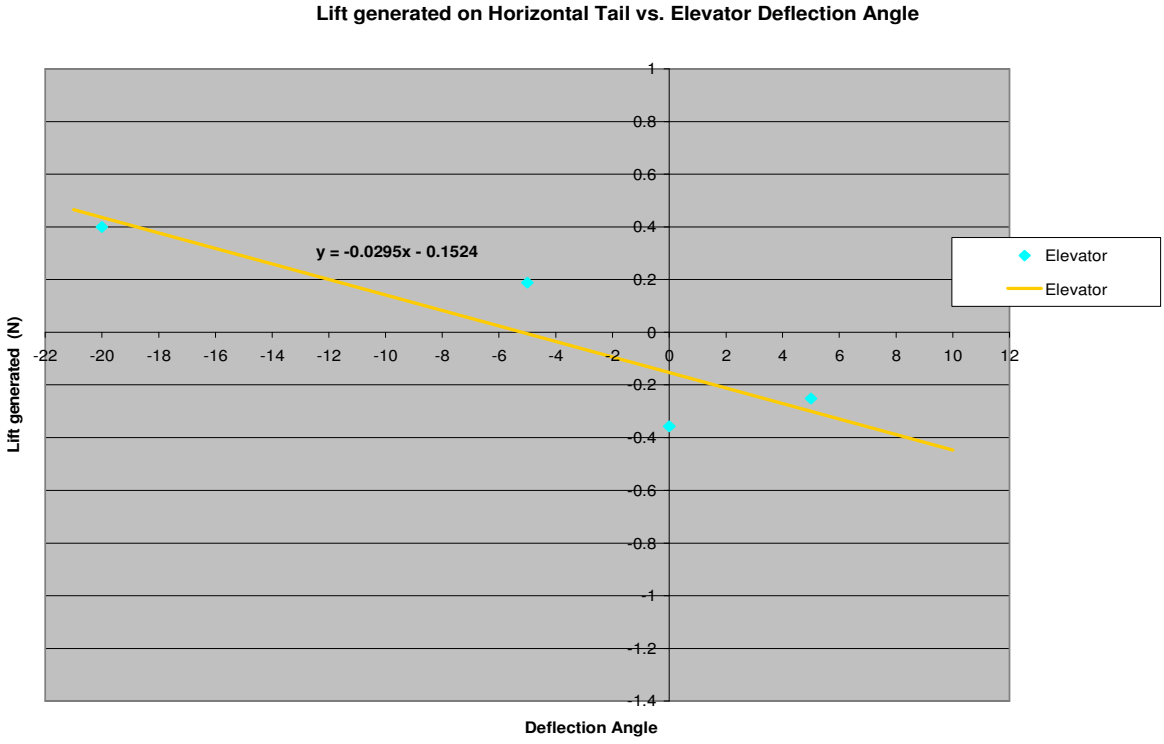

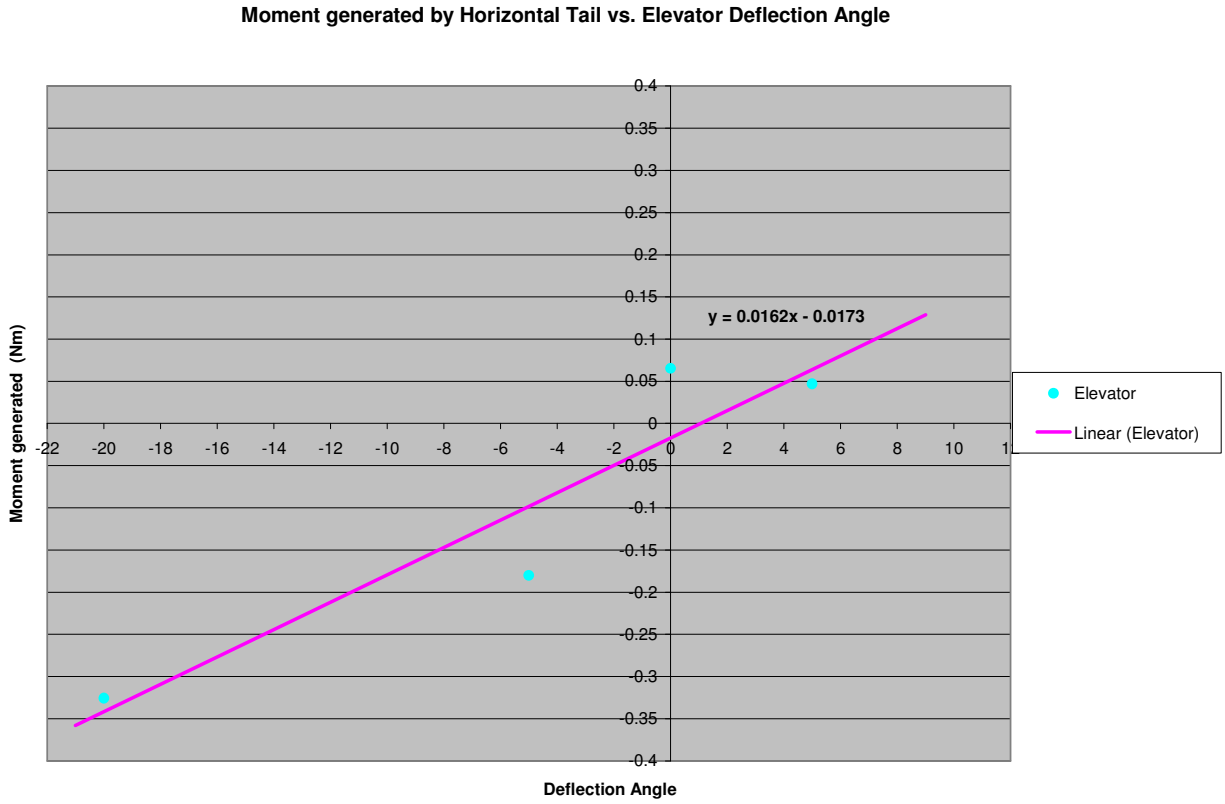
Moment generated by Horizontal Tail vs. Elevator Deflection Angle
Moment generated (Nm)
Deflection Angle
y = 0.0162x - 0.0173
Elevator
Linear (Elevator)
0.4
0.35
0.3
0.25
0.2
0.15
0.1
0.05
0
-0.05
-0.1
-0.15
-0.2
-0.25
-0.3
-0.35
-0.4
-22
-20
-18
-16
-14
-12
-10
-8
-6
-4
-2
0
2
4
6
8
10

For Rudder:

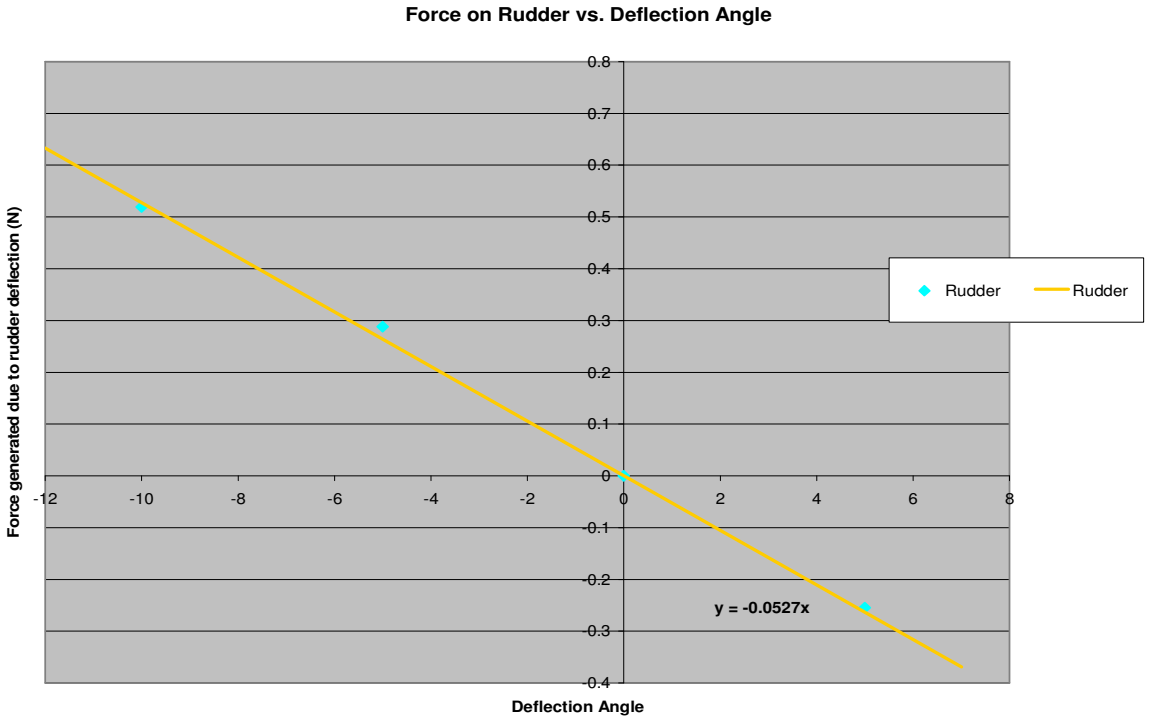
Force on Rudder vs. Deflection Angle
Force generated due to rudder deflection (N)
Deflection Angle
y = -0.0527x
Rudder
Rudder
0.8
0.7
0.6
0.5
0.4
0.3
0.2
0.1
0
-0.1
-0.2
-0.3
-0.4
-12
-10
-8
-6
-4
-2
0
2
4
6
8

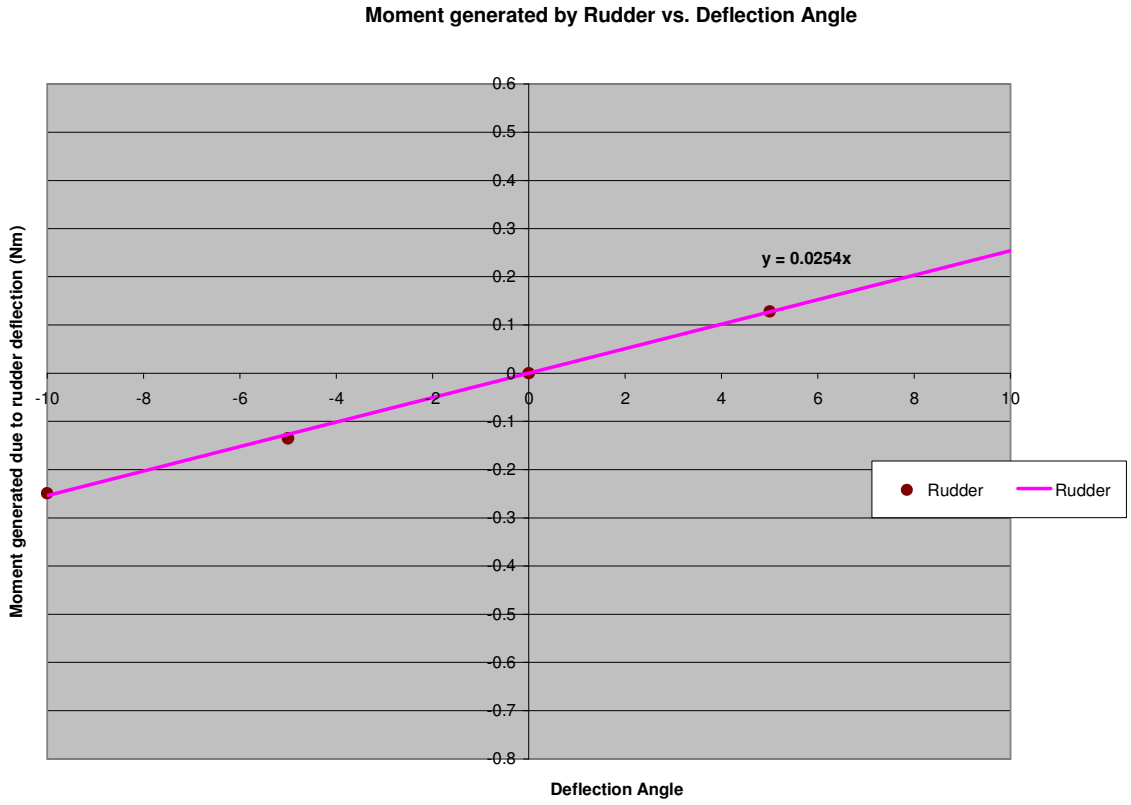
Moment generated by Rudder vs. Deflection Angle
Moment generated due to rudder deflection (Nm)
Deflection Angle
y = 0.0254x
Rudder
Rudder
0.6
0.5
0.4
0.3
0.2
0.1
0
-0.1
-0.2
-0.3
-0.4
-0.5
-0.6
-0.7
-0.8
-10
-8
-6
-4
-2
0
2
4
6
8
10

Appendix B: Servo Specifications

ANNOUNCED SPECIFICATIONS OF HS−85MG+ MIGHT MICRO METAL GEAR SERVO

1.TECHNICAL VALUES

CONTROL SYSTEM	:+PULSE WIDTH CONTROL 1500usec NEUTRAL	
OPERATING VOLTAGE RANGE	:4.8V TO 6.0V	
OPERATING TEMPERATURE RANGE	:-20°C TO +60°C	
TEST VOLTAGE	:AT 4.8V AT 6.0V	
OPERATING SPEED	:0.16sec/60° AT NO LOAD	0.14sec/60° AT NO LOAD
STALL TORQUE	:3.0kg.cm(41.66oz.in)	3.5kg.cm(48.60oz.in)
OPERATING ANGLE	:40°/ONE SIDE PULSE TRAVELING 400usec	
DIRECTION	:CLOCK WISE/PULSE TRAVELING 1500 TO 1900usec	
CURRECT DRAIN	:8mA/IDLE AND 240mA NO LOAD RUNNING	
DEAD BAND WIDTH	:8usec	
CONNECTOR WIRE LENGTH	:160mm (6.29in)	
DIMENSIONS	:29x13x30mm (1.14x0.51x1.18in)	
WEIGHT	:21.9g (0.77oz)	

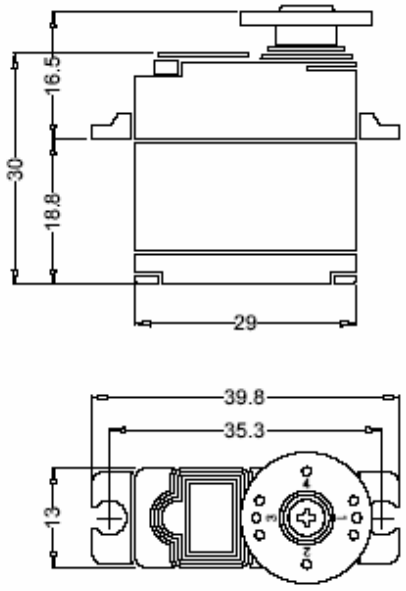

2.FEATURES

3-POLES FERRITE MOTOR
ONE BALL BEARING
DIRECT POTENTIOMETER DRIVE
HYBRID I.C
4-METAL GEARS

3.APPLICATIONS

FAST ELECTRIC BOATS
ROCKET PLANES AND SAILPLANE WINGS

Appendix C: Microcontroller and Sensor Specifications

Stamp Specifications (revised 04/05)

Released Products	Rev.Dx / BS1-IC	BS2-IC	BS2e-IC	BS2sx-IC
Package	PCB w/Proto / 14-pin SIP	24-pin DIP	24-pin DIP	24-pin DIP
Package Size (L x W x H)	2.5" x 1.5" x .5" / 1.4" x .6" x .1"	1.2" x 0.6" x 0.4"	1.2" x 0.6" x 0.4"	1.2" x 0.6" x 0.4"
Environment *	0° - 70° C (32° - 158° F) **	0° - 70° C (32° - 158° F) **	0° - 70° C (32° - 158° F)	0° - 70° C (32° - 158° F)
Microcontroller	Microchip PIC16C56a	Microchip PIC16C57c	Ubicom SX28AC	Ubicom SX28AC
Processor Speed	4 MHz	20 MHz	20 MHz	50 MHz
Program Execution Speed	~2,000 instructions/sec.	~4,000 instructions/sec.	~4,000 instructions/sec.	~10,000 instructions/sec.
RAM Size	16 Bytes (2 I/O, 14 Variable)	32 Bytes (6 I/O, 26 Variable)	32 Bytes (6 I/O, 26 Variable)	32 Bytes (6 I/O, 26 Variable)
Scratch Pad RAM	N/A	N/A	64 Bytes	64 Bytes
EEPROM (Program) Size	256 Bytes, ~80 Instructions	2K Bytes, ~500 Instructions	8 x 2K Bytes, ~4,000 Inst.	8 x 2K Bytes, ~4,000 Inst.
Number of I/O pins	8	16 + 2 Dedicated Serial	16 + 2 Dedicated Serial	16 + 2 Dedicated Serial
Voltage Requirements	5 - 15 vdc	5 - 15 vdc	5 - 12 vdc	5 - 12 vdc
Current Draw @ 5V	1 mA Run / 25 µA Sleep	3 mA Run / 50 µA Sleep	25 mA Run / 200 µA Sleep	60 mA Run / 600 µA Sleep
Source / Sink Current per I/O	20 mA / 25 mA	20 mA / 25 mA	30 mA / 30 mA	30 mA / 30 mA
Source / Sink Current per unit	40 mA / 50 mA	40 mA / 50 mA per 8 I/O pins	60 mA / 60 mA per 8 I/O pins	60 mA / 60 mA per 8 I/O pins
PBASIC Commands***	32	42	45	45
PC Programming Interface	Serial (w/BS1 Serial Adapter)	Serial (9600 baud)	Serial (9600 baud)	Serial (9600 baud)
Windows Text Editor	Stampw.exe (v2.1 and up)	Stampw.exe (v1.04 and up)	Stampw.exe (v1.096 and up)	Stampw.exe (v1.091 and up)

Released Products	BS2p24-IC	BS2p40-IC	BS2pe-IC	BS2px-IC	Javelin Stamp
Package	24-pin DIP	40-pin DIP	24-pin DIP	24-pin DIP	24-pin DIP
Package Size (L x W x H)	1.2" x 0.6" x 0.4"	2.1" x 0.6" x 0.4"	1.2" x 0.6" x 0.4"	1.2" x 0.6" x 0.4"	1.24" x 0.60" x 0.45"
Environment *	0° - 70° C (32° - 158° F)	0° - 70° C (32° - 158° F)	0° - 70° C (32° - 158° F)	0° - 70° C (32° - 158° F)	0° - 70° C (32° - 158° F)
Microcontroller	Ubicom SX48AC	Ubicom SX48AC	Ubicom SX48AC	Ubicom SX48AC	Ubicom SX48AC
Processor Speed	20 MHz Turbo	20 MHz Turbo	8 MHz Turbo	32 MHz Turbo	25 MHz Turbo
Program Execution Speed	~12,000 Instructions/sec.	~12,000 Instructions/sec.	~6000/sec.	~19,000 Instructions/sec.	~8,500 Instructions/sec.
RAM Size	38 Bytes (12 I/O, 26 Variable)	38 Bytes (12 I/O, 26 Variable)	38 Bytes (12 I/O, 26 Variable)	38 Bytes (12 I/O, 26 Variable)	32768 Bytes
Scratch Pad RAM	128 Bytes	128 Bytes	128 Bytes	128 Bytes	N/A
EEPROM (Program) Size	8 x 2K Bytes, ~4,000 Inst.	8 x 2K Bytes, ~4,000 Inst.	16 x 2K Bytes (16 K for source)	8 x 2K Bytes, ~4,000 Inst.	32768 Bytes
Number of I/O pins	16 + 2 Dedicated Serial	32 + 2 Dedicated Serial	16 + 2 Dedicated Serial	16 + 2 Dedicated Serial	16
Voltage Requirements	5 - 12 vdc	5 - 12 vdc	5 - 12 vdc	5 - 12 vdc	5 - 24 vdc
Current Draw @ 5V	40 mA Run / 350 µA Sleep	40 mA Run / 350 µA Sleep	15 mA Run / 36 µA Sleep	55 mA Run / 450 µA Sleep	80 mA Run / No Sleep
Source / Sink Current per I/O	30 mA / 30 mA	30 mA / 30 mA	30 mA / 30 mA	30 mA / 30 mA	30 mA / 30 mA
Source / Sink Current per unit	60 mA / 60 mA per 8 I/O pins	60 mA / 60 mA per 8 I/O pins	60 mA / 60 mA per 8 I/O pins	60 mA / 60 mA per 8 I/O pins	60 mA / 60 mA per 8 I/O pins
PBASIC Commands***	51	61	61	63	0 (Java)
PC Programming Interface	Serial (9600 baud)	Serial (9600 baud)	Serial (9600 baud)	Serial (19200 baud)	Serial (28800 baud)
Windows Text Editor	Stampw.exe (v1.1 and up)	Stampw.exe (v1.1 and up)	Stampw.exe (v1.33 and up)	Stampw.exe (v2.2 and up)	Javelin Stamp IDE

* 70% Non-Condensing Humidity
** Industrial Models Available, -40° - 85° C (-40° - 185° F). Contact Parallax Sales for information.
*** Using PBASIC 2.5 for BS2-type models.

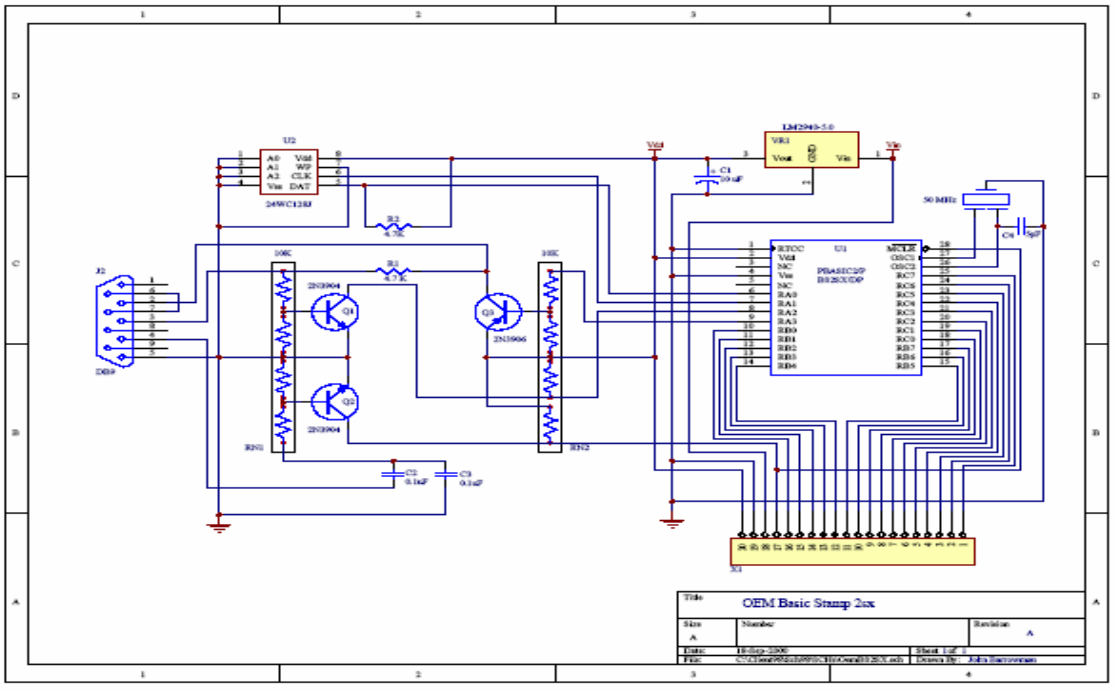

BASIC Stamp 2sx – IC Schematic Drawing

PARALLAX
599 Menlo Drive, Suite 100
Rocklin, California 95765, USA
Office: (916) 624-8333
Fax: (916) 624-8003

Sales: sales@parallax.com
Tech Support: support@parallax.com
Web Site: www.parallax.com
Educational: www.stampsinclass.com

Board Of Education® Rev C (#28150)

Development / Education Platform for the BASIC Stamp® and Javelin Stamp Microcontrollers

The Board Of Education (BOE) is a complete, low-cost development platform designed for those interested in learning and using Parallax's 24-pin BASIC Stamp or Javelin Stamp modules. Its compact size, convenient features, and low price make it an ideal tool for the student and educator. The BOE is a great tool with which to get started with Parallax BASIC Stamp ICs. For educators, the BOE provides a clean, efficient platform for our Stamps In Class Parts and Text Kits, or your own BASIC Stamp-based curriculum.

Features

- 2.1 mm center-positive plug and 9-volt battery power supply connections, mechanically interlocked to prevent dual connection.
- Three-position power switch allows BASIC Stamp IC programming without providing power to servo connectors.
- Jumper selection of servo power: regulated (Vdd) or unregulated (Vin).
- Serial (DB-9) connector for BASIC Stamp IC programming and serial communication during run-time.
- On-board regulator delivers up to 1 amp of power for larger projects.
- P0 - P15 I/O pins, Vdd, Vin, and Vss connections brought adjacent to 2" x 1 3/8" breadboard area.
- Female 10-pin dual row connector for optional AppMods.

Packing List

• Board of Education Rev C	#800-28850
• Pack of 3" jumper wires	#800-00016
• PCB rubber feet	#700-00037
• Documentation	

Mechanical Dimensions

• PCB	4.00" x 3.05" (102 mm x 77 mm)
• Mounting Holes	3.75" x 2.75" (95 mm x 70 mm)

Board of Education – Top View (without BASIC Stamp module)

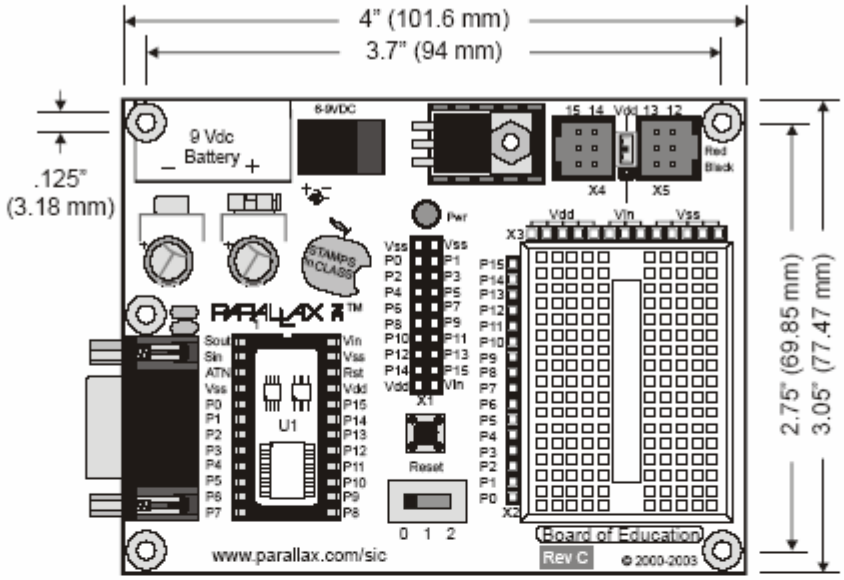

Using the BOE Breadboard

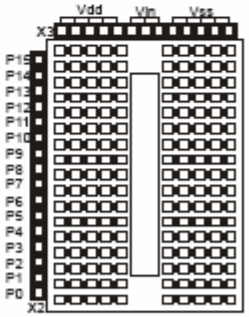

The breadboard has many strips of copper which run underneath the board in a horizontal fashion. These strips connect the sockets to each other. This makes it easy to connect components together to build circuits.

To use the breadboard, the legs of components or wires are placed in the sockets. The sockets are made so that they will hold the component in place. Each hole is connected to one of the metal strips running underneath the board. Each metal strip forms a node. A node is a point in a circuit where two components are connected. Connections between different components are formed by putting their legs in a common node. There are two columns of 17 nodes on the breadboard. Each node contains five holes.

For chips with many legs (ICs), place them in the middle of the board so that half of the legs are on the left side and half are on the right side. Nodes on the left side are not connected to nodes on the right side.

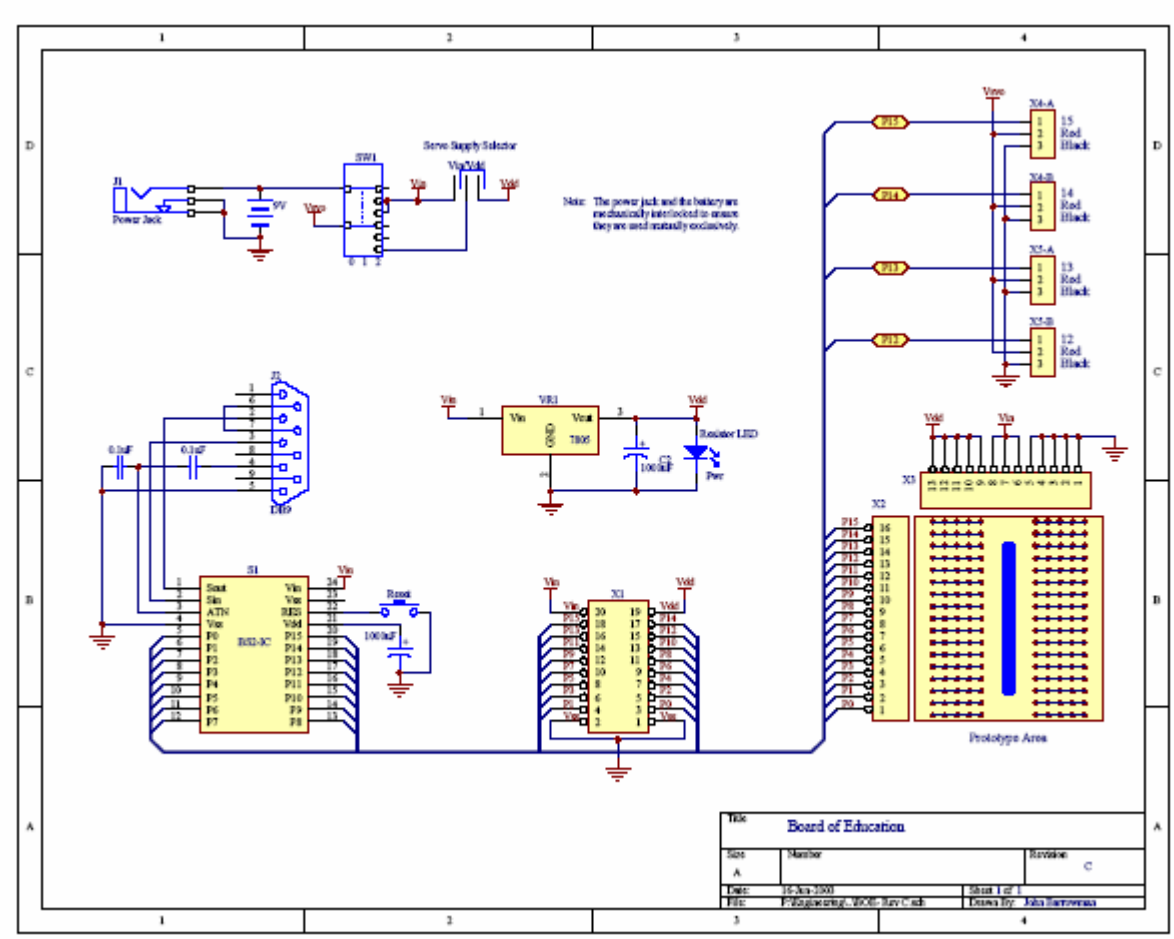

Board of Education Schematic Drawing

PARALLAX

599 Menlo Drive, Suite 100
Rocklin, California 95765, USA
Office: (916) 624-8333
Fax: (916) 624-8003

General: info@parallax.com
Technical: support@parallax.com
Web Site: www.parallax.com
Educational: www.stampsinclass.com

PING)))™ Ultrasonic Range Finder (#28015)

The Parallax PING))) ultrasonic range finder provides precise, non-contact distance measurements from about 3 cm (1.2 inches) to 3 meters (3.3 yards). It is very easy to connect to BASIC Stamp or Javelin Stamp microcontrollers, requiring only one I/O pin.

The Ping sensor works by transmitting an ultrasonic (well above human hearing range) burst and providing an output pulse that corresponds to the time required for the burst echo to return to the sensor. By measuring the echo pulse width the distance to target can easily be calculated.

Features

- Supply Voltage – 5 vdc
- Supply Current – 30 mA typ; 35 mA max
- Range – 3 cm to 3 m (1.2 in to 3.3 yrds)
- Input Trigger – positive TTL pulse, 2 uS min, 5 uS typ.
- Echo Pulse – positive TTL pulse, 115 uS to 18.5 mS
- Echo Hold-off – 750 uS from fall of Trigger pulse
- Burst Frequency – 40 kHz for 200 uS
- Burst Indicator LED shows sensor activity
- Delay before next measurement – 200 uS
- Size – 22 mm H x 46 mm W x 16 mm D (0.84 in x 1.8 in x 0.6 in)

Dimensions

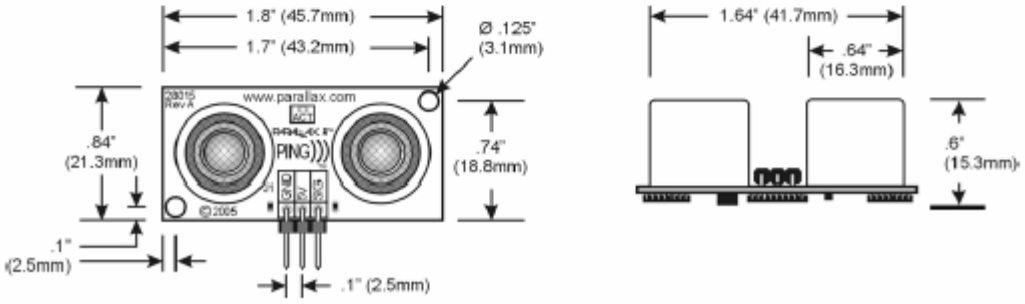

Connection to a Microcontroller

The PING))) sensor has a male 3-pin header used to supply power (5 vdc), ground, and signal. The header allows the sensor to be plugged into a solderless breadboard, or to be located remotely through the use of a standard servo extender cable. Standard connections are show in the diagram below:

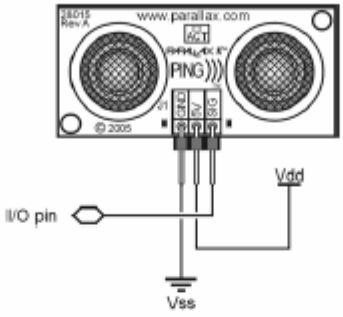

Theory of Operation

The Ping sensor detects objects by emitting a short ultrasonic burst and then "listening" for the echo. Under control of a host microcontroller (trigger pulse), the sensor emits a short 40 kHz (ultrasonic) burst. This burst travels through the air at about 1130 feet per second, hits an object and then bounces back to the sensor. The PING))) sensor provides an output pulse to the host that will terminate when the echo is detected, hence the width of this pulse corresponds to the distance to the target.

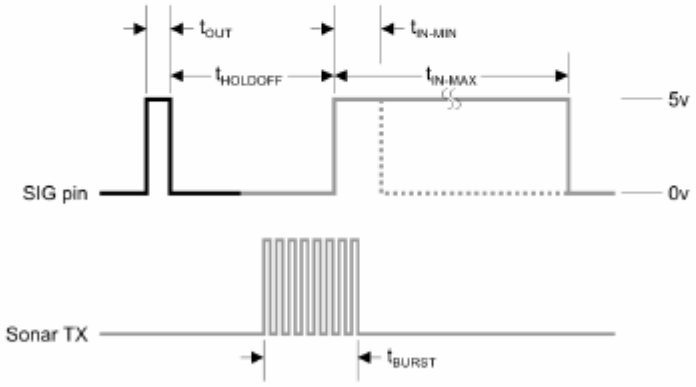

HOST	t_{OUT}	2 uS (min), 5 uS typical
PING	$t_{HOLDOFF}$	750 uS
	t_{BURST}	200 uS @ 40 kHz
	t_{IN-MIN}	115 uS
	t_{IN-MAX}	18.5 mS

Test Data

The following test data is based on the PING))) sensor, tested in the Parallax lab, while connected to a BASIC Stamp microcontroller module. The test surface was a linoleum floor, so the sensor was elevated to minimize floor reflections in the data. All tests were conducted at room temperature, indoors, in a protected environment. The target was always centered at the same elevation as the PING))) sensor.

Test 1

Sensor Elevation: 40 in. (101.6 cm)
Target: 3.5 in. (8.9 cm) diameter cylinder, 4 ft. (121.9 cm) tall – vertical orientation

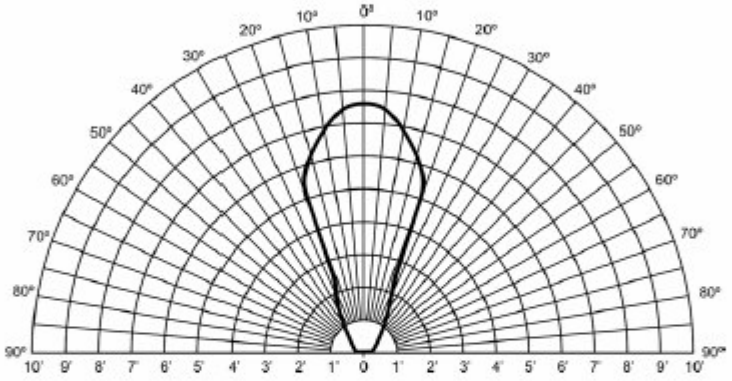

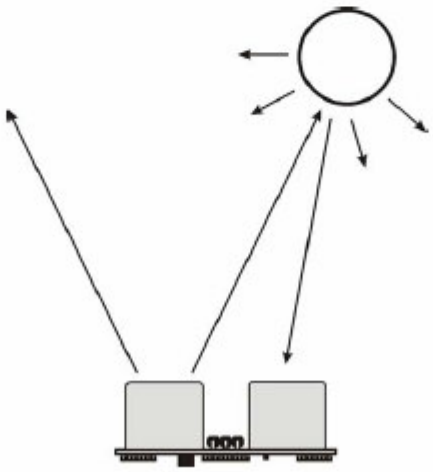

Test 2

Sensor Elevation: 40 in. (101.6 cm)
Target: 12 in. x 12 in. (30.5 cm x 30.5 cm) cardboard, mounted on 1 in. (2.5 cm) pole
- target positioned parallel to backplane of sensor

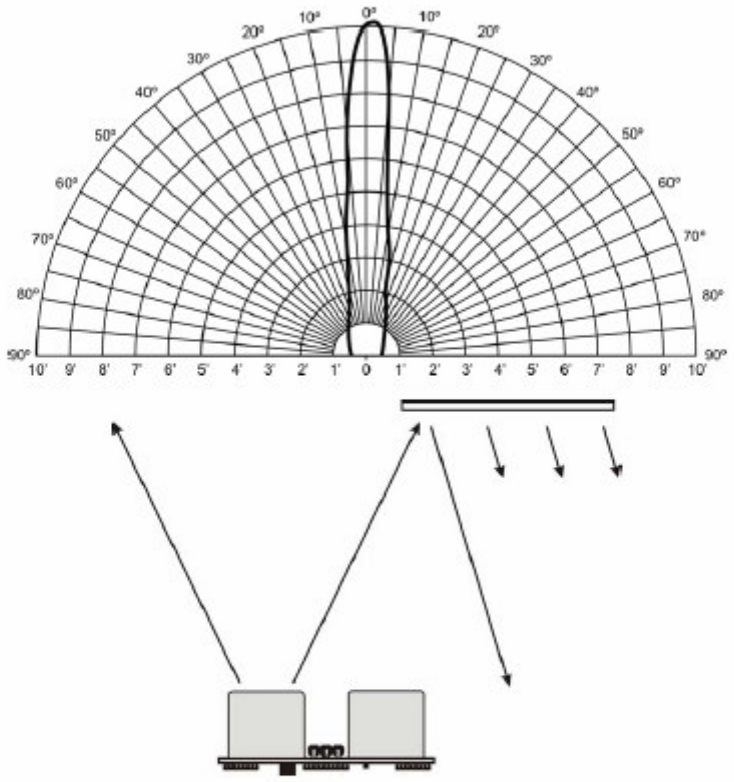

Appendix D: TXBasic Code for TattleTale Data Logger

```
print
print "*****************************************************"
print "*                                                   *"
print "* This program is used to measure the output of the servo *"
print "*                                                   *"
print "*****************************************************"
print
enterch:
        print
        input "What channel is the Potentiometer connected to (0 or 7)? "potential
        iff potential < 0 | potential > 7
                print
                print "The channel must be between 0 and 7 to work!"
                goto enterch
        endif
readings:
        print
        input "How many Potentiometer readings do you want to take? "numread
        print
        print "Do you wish to start? (Y/N)";
        gosub getch
        if answer = &h79 goto start
start:
        sleep 0                 // Suppresses the * before the first reading
        for x = 1 to numread
                print "Reading Number ", x
                sleep 2
                pop = (chan(potential))
                print "The Reading is ", #05f, pop, " Volts"
                print
        next x
print
print "Do you want to continue? (Y/N) ";  // allows using characters
gosub getch
if answer = &h79 goto readings
print
print "*******************************************"
print "*                                         *"
print "* End of program. Thank you.*"
print "*                                         *"
print "*******************************************"
stop


// This subroutine checks the serial port for the next in-coming character
// and converts it to lower-case. It then echoes the character and returns
// the character in variable 'answer'.
getch: y = 0
```

```
wait:   itext y,0
        if y = 0 goto wait              // waits until a is key pressed
        y = 0
        answer = get(y) | &h20                  // convert to upper case
        print \answer                   // echo the answer
        return
End code
```

Appendix E: Microcontroller Programming Source Codes

E-1: Program for Servo Calibration

E-2: Program for Testing Activation Command

E-3: Program for Sensor Readings

E-4: Program for Reading, Storing and Displaying Data

E-5: Program for Automatic Height Control Function

Appendix E-1: Program for Servo Calibration

```
'This program is written for configuring the servo. By varying the input pulse, it determines
the corresponding angle of deflection on the servo and test for its responsiveness

' {$STAMP BS2sx}
' {$PBASIC 2.5}


pulseWidth      VAR   Word
ElevServo       CON   12

FREQOUT 2, 2000, 3000          ' Signal program start/reset.

DEBUG "Start"

DO

   DEBUG "Enter pulse width: "   ' vary pulse width to calibrate servo

   DEBUGIN DEC pulseWidth

   PULSOUT ElevServo, pulseWidth

   PAUSE 10

LOOP
```

Table 5: Servo calibration readings

Input Readings	Pulse Width (ms)	Servo Deflection Angle (°)	Direction
1875	1.500	0	No Rotation
1925	1.540	3	CW
2075	1.660	12	CW
2125	1.700	15	CW
2175	1.740	18	CW
1825	1.460	3	CCW
1675	1.340	12	CCW
1475	1.180	24	CCW
1375	1.100	30	CCW

Appendix E-2: Program for Testing Activation Command

```
'This program is written to test out the difference in reading between an On and Off state
command from the remote controller. Channel 5 on the remote controller is used as the
dedicated on/off relay switch.

' {$STAMP BS2sx}
' {$PBASIC 2.5}

Ch5       CON  15    'Activation input

Elev    VAR  Word


DO

  PULSIN Ch5,1,Elev     ' Read activation command

  DEBUG CR, "The reading is: "

  DEBUG SDEC Elev

  PAUSE 2000

LOOP
```

Appendix E-3: Program for Sensor Readings

'This program is written to obtain altitude readings while the aircraft is in flight. Note that the interval at which the height readings at taken can be adjusted accordingly.

```
' {$STAMP BS2sx}
' {$PBASIC 2.5}

' -----[ DATA Directives ]-------------------------------------------------

Records       DATA    (101)
RecordsEnd    DATA

' -----[ I/O Definitions ]-------------------------------------------------

Ping          PIN     15

' -----[ Constants ]------------------------------------------------------

#SELECT $STAMP
  #CASE BS2, BS2E
    Trigger     CON     5                 ' trigger pulse = 10 uS
    Scale       CON     $200               ' raw x 2.00 = uS
  #CASE BS2SX, BS2P, BS2PX
    Trigger     CON     13
    Scale       CON     $0CD               ' raw x 0.80 = uS
  #CASE BS2PE
    Trigger     CON     5
    Scale       CON     $1E1               ' raw x 1.88 = uS
#ENDSELECT

RawToIn       CON     889                 ' 1 / 73.746 (with **)
RawToCm       CON     2257                ' 1 / 29.034 (with **)

IsHigh        CON     1                 ' for PULSOUT
IsLow         CON     0

' -----[ EEPROM Data ]----------------------------------------------------

FREQOUT 2, 5000, 4000

' -----[ Variables ]------------------------------------------------------

char          VAR     Byte
eeIndex       VAR     Word
value         VAR     Word
rawDist       VAR     Word                ' raw measurement
inches        VAR     Word
cm            VAR     Word
```

```
' -----[ Initialization ]----------------------------------------------

Reset:
  DEBUG CLS,                              ' setup report screen
        "Parallax Ping Sonar  ", CR,
        "====================", CR,
        CR,
        "Time (uS).....       ", CR,
        "Inches.......        ", CR,
        "Centimeters...       "

' -----[ Program Code ]------------------------------------------------

Main:

FOR eeIndex = Records TO RecordsEnd STEP 2       'take 15 readings

    GOSUB Get_Sonar                         ' get sensor value
    inches = rawDist ** RawToIn              ' convert to inches
    cm = rawDist ** RawToCm                  ' convert to centimeters
    value = cm
    WRITE eeIndex, Word value

    DEBUG CRSRXY, 15, 3,                     ' update report screen
          DEC rawDist, CLREOL,
          CRSRXY, 15, 4,
          DEC inches, CLREOL,
          CRSRXY, 15, 5,
          DEC cm, CLREOL

    PAUSE 500

NEXT

   DEBUG CR, "End of records."
   FREQOUT 2, 3000, 3000

END


' -----[ Subroutines ]--------------------------------------------------

Get_Sonar:
  Ping = IsLow                           ' make trigger 0-1-0
  PULSOUT Ping, Trigger                    ' activate sensor
  PULSIN  Ping, IsHigh, rawDist            ' measure echo pulse
  rawDist = rawDist */ Scale              ' convert to uS
  rawDist = rawDist / 2                  ' remove return trip
  RETURN
```

Appendix E-4: Program for Reading, Storing and Displaying Data

```
'This program demonstrates storing, retrieving and erasing values in EEPROM memory.
' Values are obtained at pre-determined intervals using the PING sonar sensor

'{$STAMP BS2sx}
'{$PBASIC 2.5}

' -----[ DATA Directives ]-------------------------------------------------

Records       DATA    (101)
RecordsEnd    DATA


' -----[ Variables ]-------------------------------------------------------

char          VAR     Byte
eeIndex       VAR     Word
value         VAR     Word
avg           VAR     Word
total         VAR     Word
rawDist       VAR     Word              ' raw measurement
inches        VAR     Word
cm            VAR     Word
counter       VAR     Word

' -----[ I/O Definitions ]------------------------------------------------
Ping          PIN     15

' -----[ Constants ]-------------------------------------------------------

#SELECT $STAMP
  #CASE BS2, BS2E
    Trigger     CON     5               ' trigger pulse = 10 uS
    Scale       CON     $200             ' raw x 2.00 = uS
  #CASE BS2SX, BS2P, BS2PX
    Trigger     CON     13
    Scale       CON     $0CD             ' raw x 0.80 = uS
  #CASE BS2PE
    Trigger     CON     5
    Scale       CON     $1E1             ' raw x 1.88 = uS
#ENDSELECT

RawToIn       CON     889               ' 1 / 73.746 (with **)
RawToCm       CON     2257              ' 1 / 29.034 (with **)

IsHigh        CON     1                 ' for PULSOUT
IsLow         CON     0

' -----[ Main Routine ]---------------------------------------------------
```

```
DO

  DEBUG CLS,
        "Type C, R or D", CR,
        "C - Clear records", CR,
        "R - Record records", CR,
        "D - Display records", CR,
        ">"

  DEBUGIN char
  DEBUG CR

  SELECT char
    CASE "C", "c"
      GOSUB Clear_Data
    CASE "R", "r"
      GOSUB Record_Data
    CASE "D", "d"
      GOSUB Display_Data
    CASE ELSE
      DEBUG CR, "Not a valid entry.",
            CR, "Try again."
      PAUSE 1500
  ENDSELECT

LOOP

' -----[ Subroutine - Clear_Data ]-----------------------------------------

Clear_Data:
  FOR eeIndex = Records TO RecordsEnd
    WRITE eeIndex, 100
  NEXT
  DEBUG CR, "Records cleared."
  PAUSE 1000
  RETURN

' -----[ Subroutine - Record_Data ]-----------------------------------------

Record_Data:
  FOR eeIndex = Records TO RecordsEnd STEP 2
    GOSUB Get_Sonar                    ' get sensor value
    inches = rawDist ** RawToIn        ' convert to inches
    cm = rawDist ** RawToCm            ' convert to centimeters
    value = cm
    WRITE eeIndex, Word value
    DEBUG CR, "Recording..."
  NEXT
  DEBUG CR, "End of records.",
```

```
        CR, "Press Enter for menu..."
  DEBUGIN char
  RETURN

' -----[ Subroutine - Display_Data ]----------------------------------------

Display_Data:
  DEBUG CR, "Index  Record",
        CR, "-----  ------",
        CR
  FOR eeIndex = Records TO RecordsEnd STEP 2
    READ eeIndex, Word value
    DEBUG DEC eeIndex, CRSRX, 7, SDEC value, CR
  NEXT

    total = 0                       ' Initialising

  FOR eeIndex = Records TO RecordsEnd STEP 2
    READ eeIndex, Word value
    total = total + value
  NEXT

    avg = total / 50
    DEBUG CR, "The average is: "
    DEBUG SDEC avg

  DEBUG CR, "Press Enter for menu..."
  DEBUGIN char
  RETURN

' -----[ Subroutine - Get_Sonar ]----------------------------------------
Get_Sonar:
  Ping = IsLow                      ' make trigger 0-1-0
  PULSOUT Ping, Trigger               ' activate sensor
  PULSIN  Ping, IsHigh, rawDist         ' measure echo pulse
  rawDist = rawDist */ Scale          ' convert to uS
  rawDist = rawDist / 2             ' remove return trip
  PAUSE 500
  RETURN
```

Appendix E-5: Program for Automatic Height Control Function

```
'This program is used to maintain the aircraft at the ideal flying altitude of 11cm, by
controlling the elevator servo

' {$STAMP BS2sx}
' {$PBASIC 2.5}

' -----[ DATA Directives ]-------------------------------------------------

Records       DATA    (101)
RecordsEnd    DATA

' -----[ I/O Definitions ]-------------------------------------------------

Ping          PIN     15
Ch2           CON     12        ' Elevator channel
Ch5           CON     14        ' Channel used to enable autopilot
ElevServo     CON     13

' -----[ Constants ]-------------------------------------------------------

#SELECT $STAMP
  #CASE BS2, BS2E
    Trigger     CON     5                 ' trigger pulse = 10 uS
    Scale       CON     $200               ' raw x 2.00 = uS
  #CASE BS2SX, BS2P, BS2PX
    Trigger     CON     13
    Scale       CON     $0CD               ' raw x 0.80 = uS
  #CASE BS2PE
    Trigger     CON     5
    Scale       CON     $1E1               ' raw x 1.88 = uS
#ENDSELECT

RawToIn       CON     889                 ' 1 / 73.746 (with **)
RawToCm       CON     2257                ' 1 / 29.034 (with **)

IsHigh        CON     1                 ' for PULSOUT
IsLow         CON     0

' -----[ EEPROM Data ]----------------------------------------------------

FREQOUT 2, 1000, 3000

' -----[ Variables ]-------------------------------------------------------

char          VAR     Byte
eeIndex       VAR     Word
value         VAR     Word
rawDist       VAR     Word                ' raw measurement
```

```
inches        VAR     Word
cm            VAR     Word
counter_1     VAR     Word
counter_2     VAR     Word
counter_3     VAR     Word
counter_4     VAR     Word
counter_5     VAR     Word
Temp          VAR     Word
Elev          VAR     Word

' -----[ Initialization ]----------------------------------------------

Reset:
  DEBUG CLS,                              ' setup report screen
        "Parallax Ping Sonar  ", CR,
        "====================", CR,
        CR,
        "Time (uS).....       ", CR,
        "Inches........       ", CR,
        "Centimeters...       "


' -----[ Program Code ]-------------------------------------------------

Main:

FOR eeIndex = Records TO RecordsEnd STEP 2

    GOSUB Get_Sonar                       ' get sensor value
    inches = rawDist ** RawToIn            ' convert to inches
    cm = rawDist ** RawToCm                ' convert to centimeters
    value = cm
    WRITE eeIndex, Word value

    DEBUG CRSRXY, 15, 3,                   ' update report screen
          DEC rawDist, CLREOL,
          CRSRXY, 15, 4,
          DEC inches, CLREOL,
          CRSRXY, 15, 5,
          DEC cm, CLREOL

    PULSIN Ch2,1,Elev    ' Read Elevator command
    PULSIN Ch5,1,Temp    ' Read enable command

    IF (Temp > 1800) THEN
      GOSUB Enabled

    ELSE
      PULSOUT ElevServo,Elev
    ENDIF
```

```
    PAUSE 500

NEXT

   DEBUG CR, "End of records."

END


' -----[ Subroutines ]------------------------------------------------


Get_Sonar:
  Ping = IsLow                          ' make trigger 0-1-0
  PULSOUT Ping, Trigger                    ' activate sensor
  PULSIN  Ping, IsHigh, rawDist             ' measure echo pulse
  rawDist = rawDist */ Scale              ' convert to uS
  rawDist = rawDist / 2                  ' remove return trip
  RETURN

Enabled:
  IF (cm = 10) THEN
     GOSUB Elevator_neutral

   ELSEIF (cm = 11) OR (cm = 12) THEN
     GOSUB Elevator_down_1

   ELSEIF (cm > 13) THEN
     GOSUB ELevator_down_2

   ELSEIF (cm = 9) OR (cm = 8) THEN
     GOSUB Elevator_up_1

   ELSEIF (cm < 7) THEN
     GOSUB Elevator_up_2

   ELSE
     HIGH 10
     PAUSE 500
     LOW 10
     PAUSE 500

   ENDIF
  RETURN

Elevator_neutral:
FOR counter_1 = 1 TO 100
  PULSOUT ElevServo, 1875                    ' Hold servo at neutral position
  PAUSE 12
```

```
NEXT

RETURN

Elevator_down_1:
FOR counter_2 = 1 TO 100
  PULSOUT ElevServo, 1775                    ' Servo turn ccw 6 deg
  PAUSE 12
NEXT

RETURN

Elevator_down_2:
FOR counter_3 = 1 TO 100
  PULSOUT ElevServo, 1675                    ' Servo turn ccw 12 deg
  PAUSE 12
NEXT

RETURN

Elevator_up_1:
FOR counter_4 = 1 TO 100
  PULSOUT ElevServo, 1975                    ' Servo turn cw 6 deg
  PAUSE 11
NEXT

RETURN

Elevator_up_2:
FOR counter_5 = 1 TO 100
  PULSOUT ElevServo, 2075                    ' Servo turn cw 12 deg
  PAUSE 11
NEXT

RETURN
```

Appendix F: Moment of Inertia Calculation

Assuming homogenous mass distribution for all subassemblies:

Table 6: Moment of inertia calculations

Subassembly	Standard shape	Mass (kg)	Distance from ideal CG, d (m)	Dimension (m)	Moment of Inertia Eqn, I_{yy}	Moment of Inertia, I_{yy} (kgm^2)
Hull + Top Cover	Circular Cylinder (radius **a** height **h**)	0.496	0.040	**a** = 0.075 **h** = 0.81	$1/12\ M\ (h^2 + 3a^2) + Md^2$	0.0286
Horizontal Tail + Servo	Elliptical Cylinder (Major axis radius **a** Minor axis radius **b**)	0.271	0.465	**a** = 0.1075 **b** = 0.04	$¼\ M(a^2 + b^2) + Md^2$	0.0570
Battery + ESC (x 02)	Rectangular Box (depth **a** length **L**)	0.206 x 2	0.230	**a** = 0.035 **L** = 0.15	$[1/12\ M\ (a^2 + L^2) + Md^2] \times 2$	0.0226
Motor Mount	Rectangular Plate(width **a**)	0.085	0.186	**a** = 0.035	$1/12\ Ma^2 + Md^2$	0.0054
Motor + Propeller (x 02)	Circular Cylinder (radius **a** height **h**)	0.144 x 2	0.193	**a** = 0.02 **h** = 0.065	$[1/12\ M\ (h^2 + 3a^2) + Md^2] \times 2$	0.0111
Wings	Half Circular Conical Shell (base radius **r** height **h**)	0.406	0.110	**r** = 0.37 **h** = 0.76	$1/4\ Mr^2 + 1/6\ Mh^2 + Md^2$	0.0579
Total:		**2.027**				**0.183**

Appendix G: Root Locus and Bode Plot